Radio point sources

- galactic objects

Pulsars

pulsars were detected on November 28, 1967
at Cambridge
using a low-frequency system $\nu = 81$ MHz
by Bell & Hewish $\rightarrow P = 5.1$ s

pulsars show lengthening of P with time
$\dot{P} = 10^{-12}$ to 10^{-21} are typical

Discovery of Pulsars
Jocelyn Bell
Cambridge, 1967

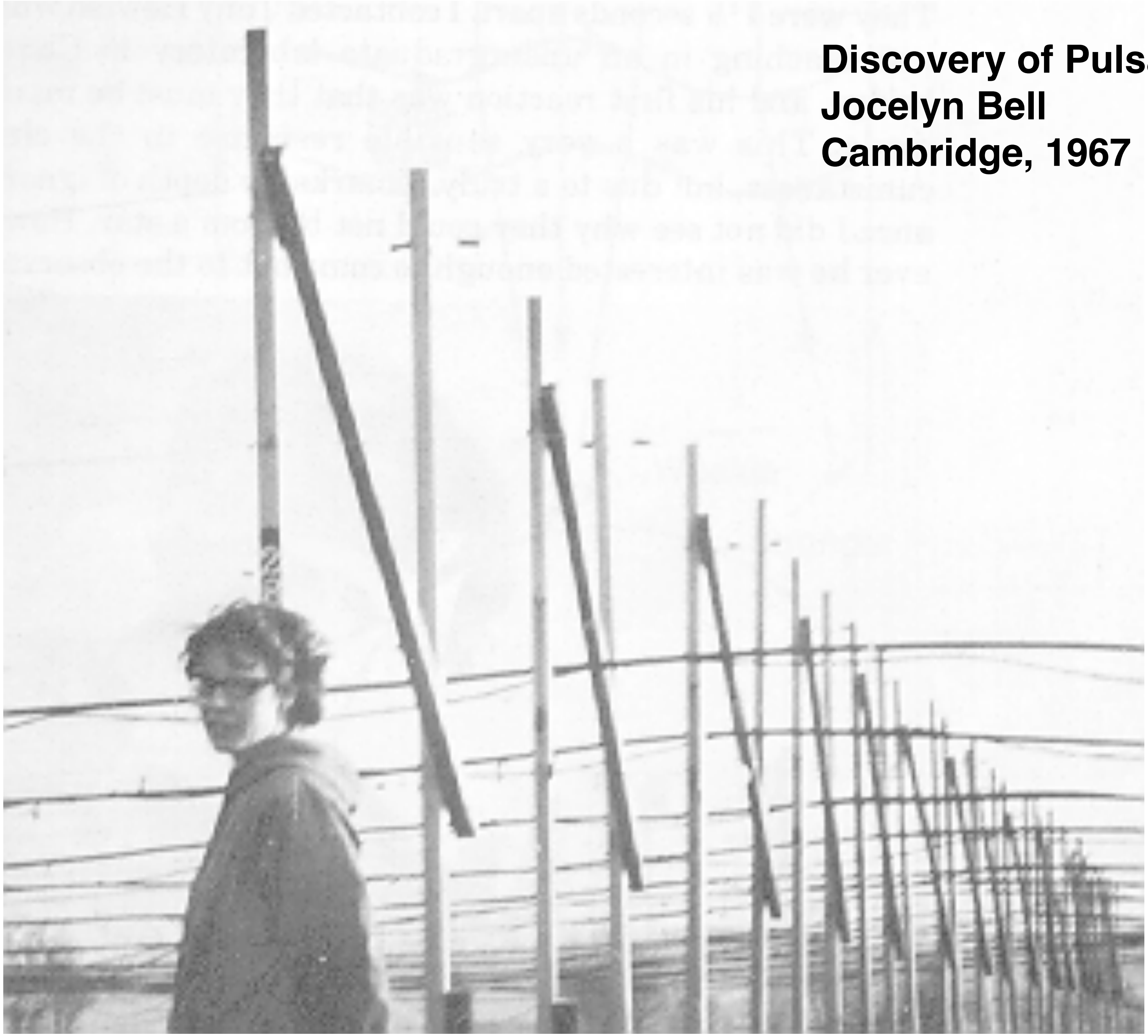

The Nobel Prize in Physics 1974

"for their pioneering research in radio astrophysics: Ryle for his observations and inventions, in particular of the aperture synthesis technique, and Hewish for his decisive role in the discovery of pulsars"

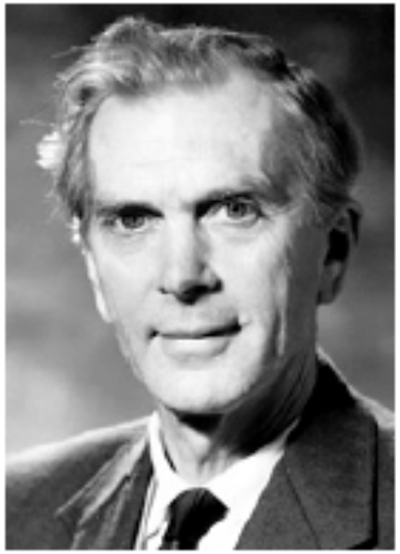

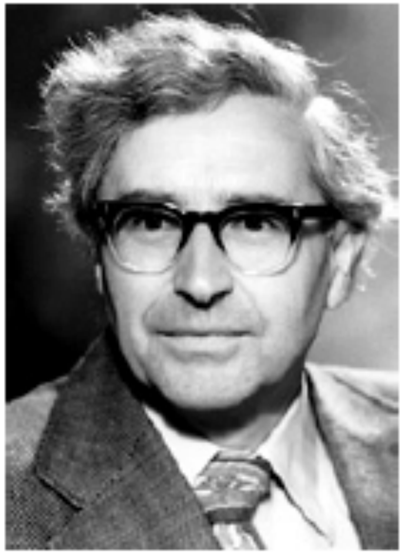

Sir Martin Ryle

1/2 of the prize

United Kingdom

University of Cambridge
Cambridge, United Kingdom

b. 1918
d. 1984

Antony Hewish

1/2 of the prize

United Kingdom

University of Cambridge
Cambridge, United Kingdom

b. 1924

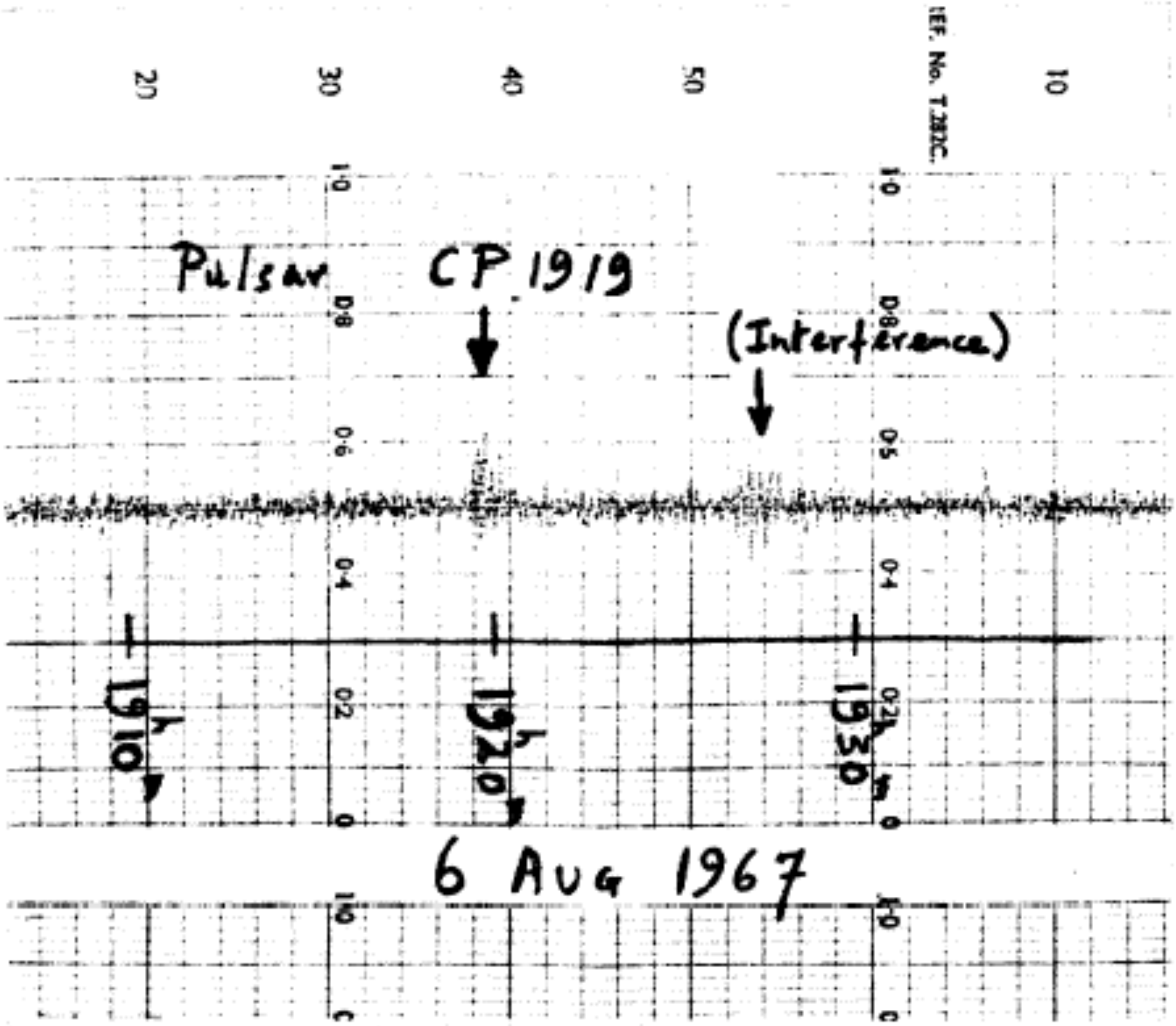

Fig. 1. The first signals from CP 1919.

pulsar is a rotating body hold together by its own gravitation

centrifugal acceleration < gravitational attraction

$$\left(\frac{2\pi}{P}\right)^2 \leq \frac{GM}{R^2} \longrightarrow \frac{\rho}{g/cm^3} \geq 1{,}41 \cdot 10^8 \left(\frac{P}{s}\right)^{-2}$$

average density

Crab pulsar $P = 0{,}033\,s \longrightarrow \rho \geq 1{,}3 \cdot 10^{11} \frac{g}{cm^3}$

density is well outside the possible range for white drafts

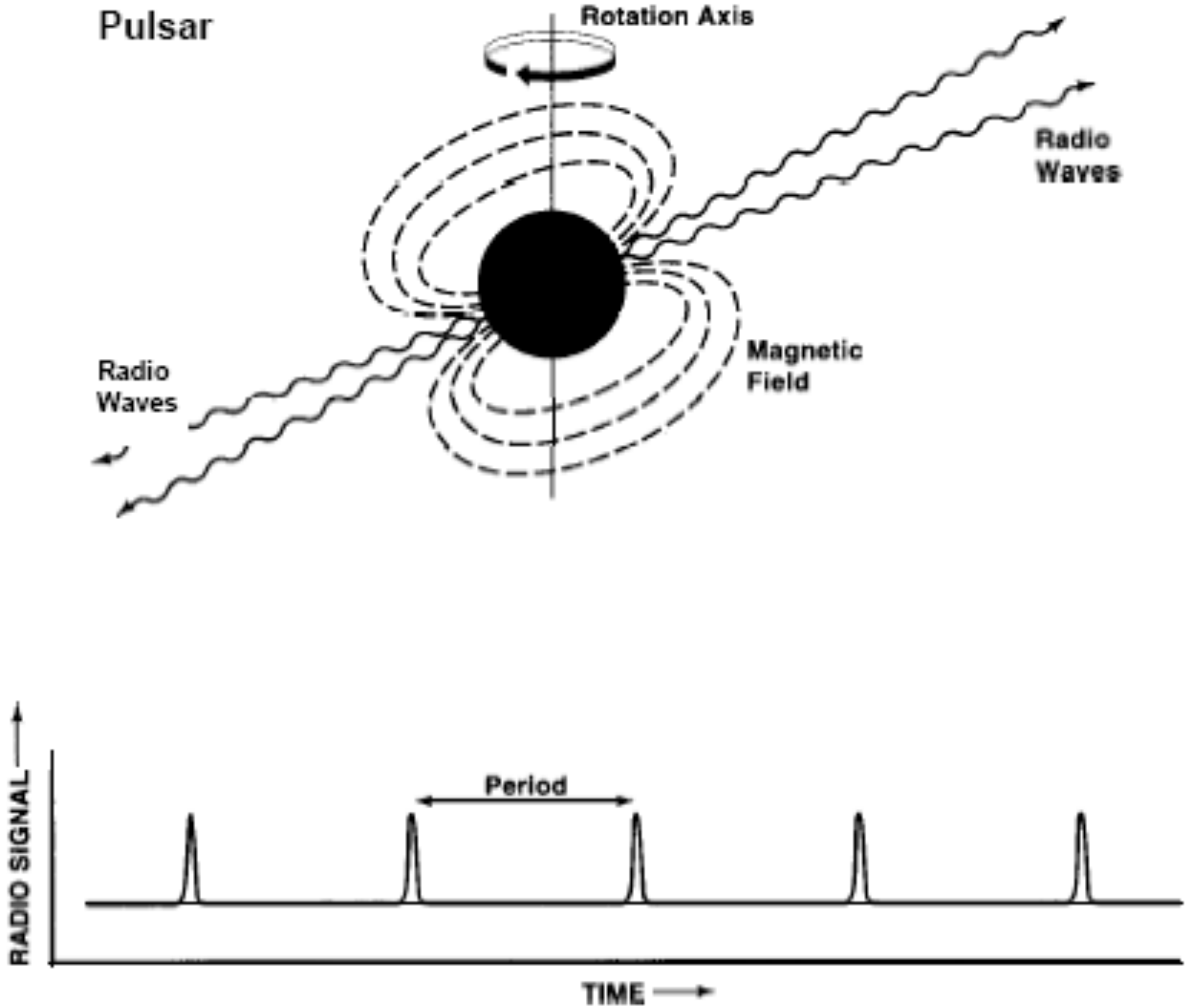

Fig. 1: A conceptual sketch of a pulsar, showing a rapidly rotating neutron star emitting narrow beams of radio waves from the polar regions of its embedded magnetic field. Also shown is a sketch of the periodic radio signal produced by a pulsar as seen by a radio telescope at the earth.

Crab Pulsar

Crab nebula (optical)

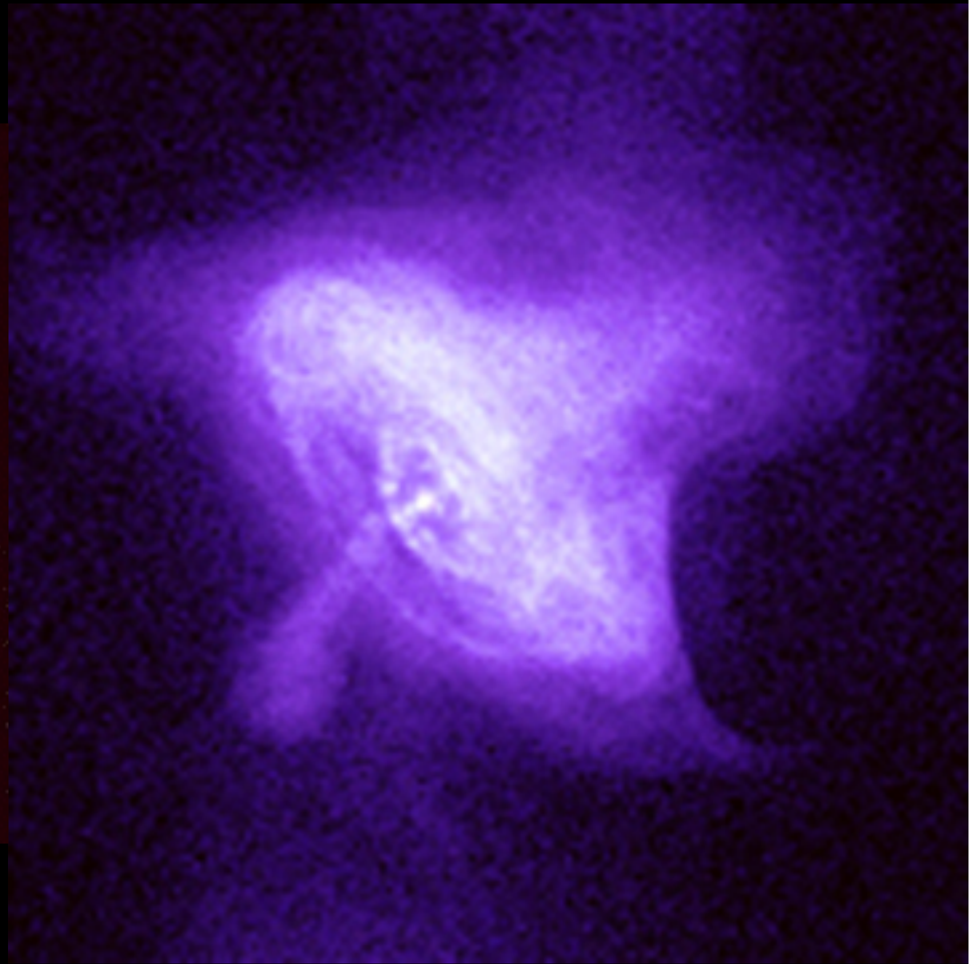

Chandra x-ray observatory

→ only neutron stars can be considered as feasible objects

$m \sim 1{,}3\ M_{\odot}$ to $2{,}1\ M_{\odot}$

$d \sim 10-20$ km

density similar to density in atomic nuclei

neutron star is formed from the collapsed remnant of a massive star, remnant of a supernova

they consist mostly of neutrons

pulsars are designated by PSR Jhhmm±ddmm

pulsating radio source followed by the position pulsars are concentrated in the galactic plane

z distribution $\rho_z(R)$ approximately exponential with scale height 600pc

$$\rho \propto \exp\left(-\frac{z}{600\,\mathrm{pc}}\right)$$

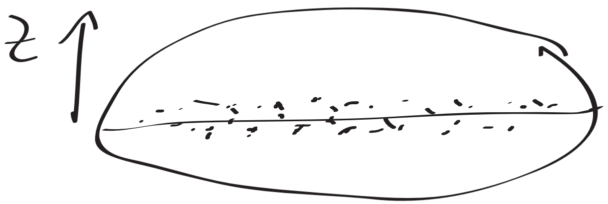

radio emission mechanism

at radius r_c the velocity is $\frac{2\pi r_c}{P} = c$

the corotating magnetic field lines reach speed of light

e.g. Crab pulsar $P = 0{,}033\,\mathrm{s}$ $r_c = 1576\,\mathrm{km}$

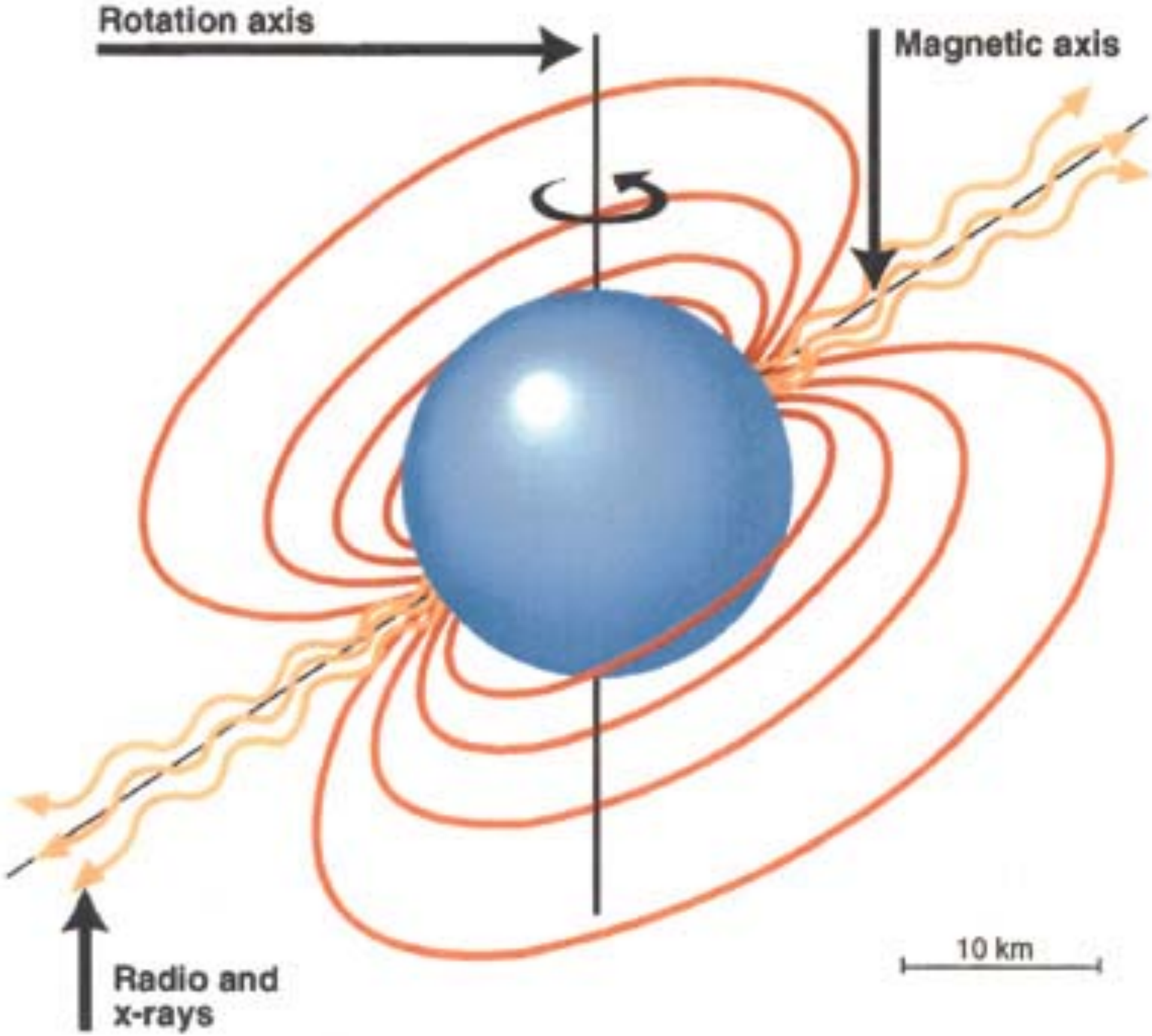

Rotation axis
Magnetic axis
Radio and x-rays
10 km

thus, the field lines cannot be closed

general idea is that radiation is emitted from the polar caps with open field lines

a fundamental problem is the high brightness temperature of pulsars, resulting in the ratio

$$\frac{kT_b}{h\nu} \approx 10^{28}$$

because of that, this region must be entirely free of matter, otherwise thermal emission occuring at frequencies with $\frac{h\nu}{kT_b} \approx 1$ (x-ray) should be observed

- extragalactic objects

Radio galaxies

among the most powerful extragalactic sources are
e.g.
Perseus A, Cygnus A, Centaurus A

most of them have active galactic nuclei (AGN)
powered by black holes
most show evidence for jets
at their ends are bright hot spots, where

Perseus A

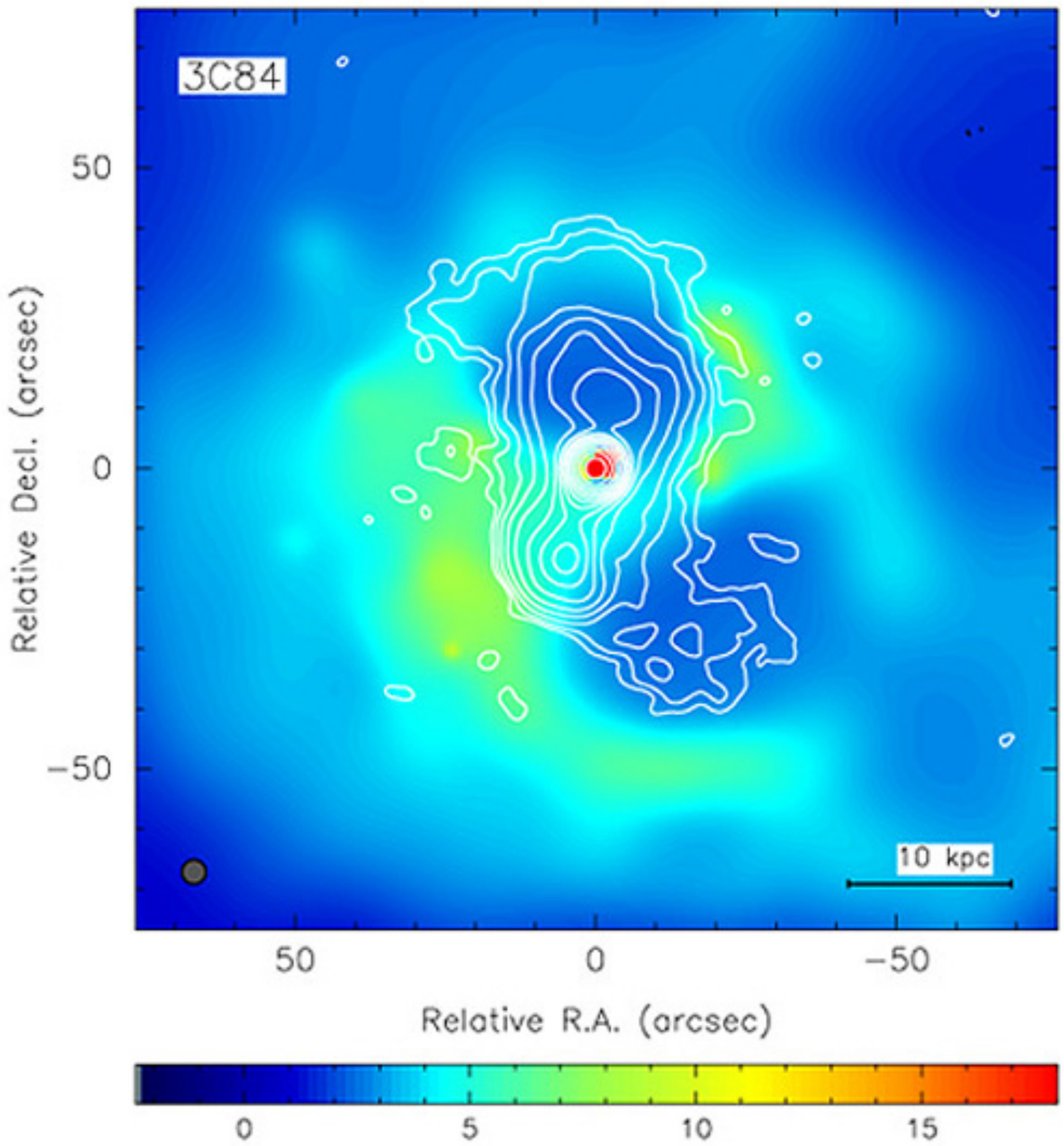

3C84
10 kpc
50
0
−50
Relative Decl. (arcsec)
50
0
−50
Relative R.A. (arcsec)
0
5
10
15

Cygnus A
(3C 405)

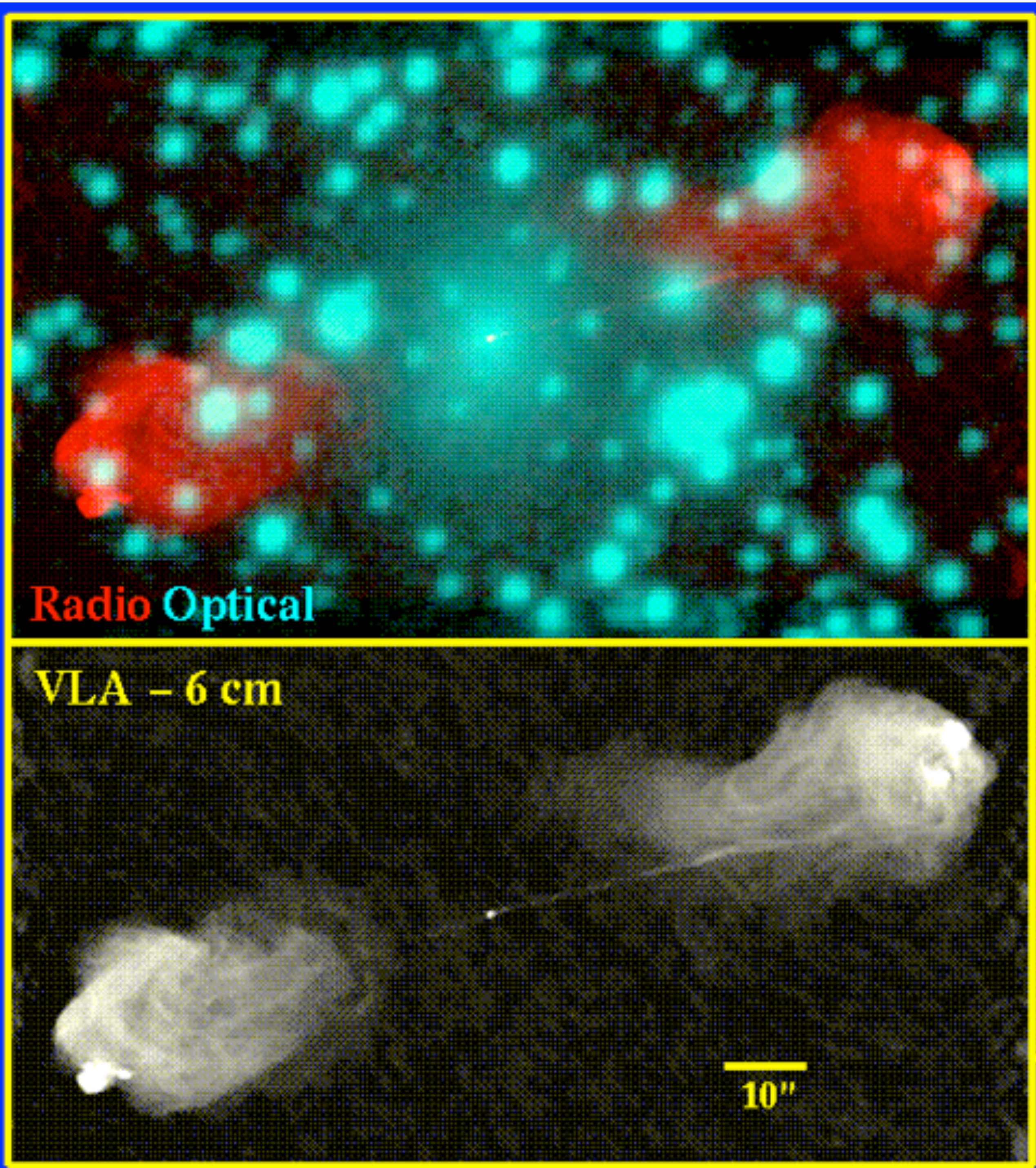

HST closeup

5″

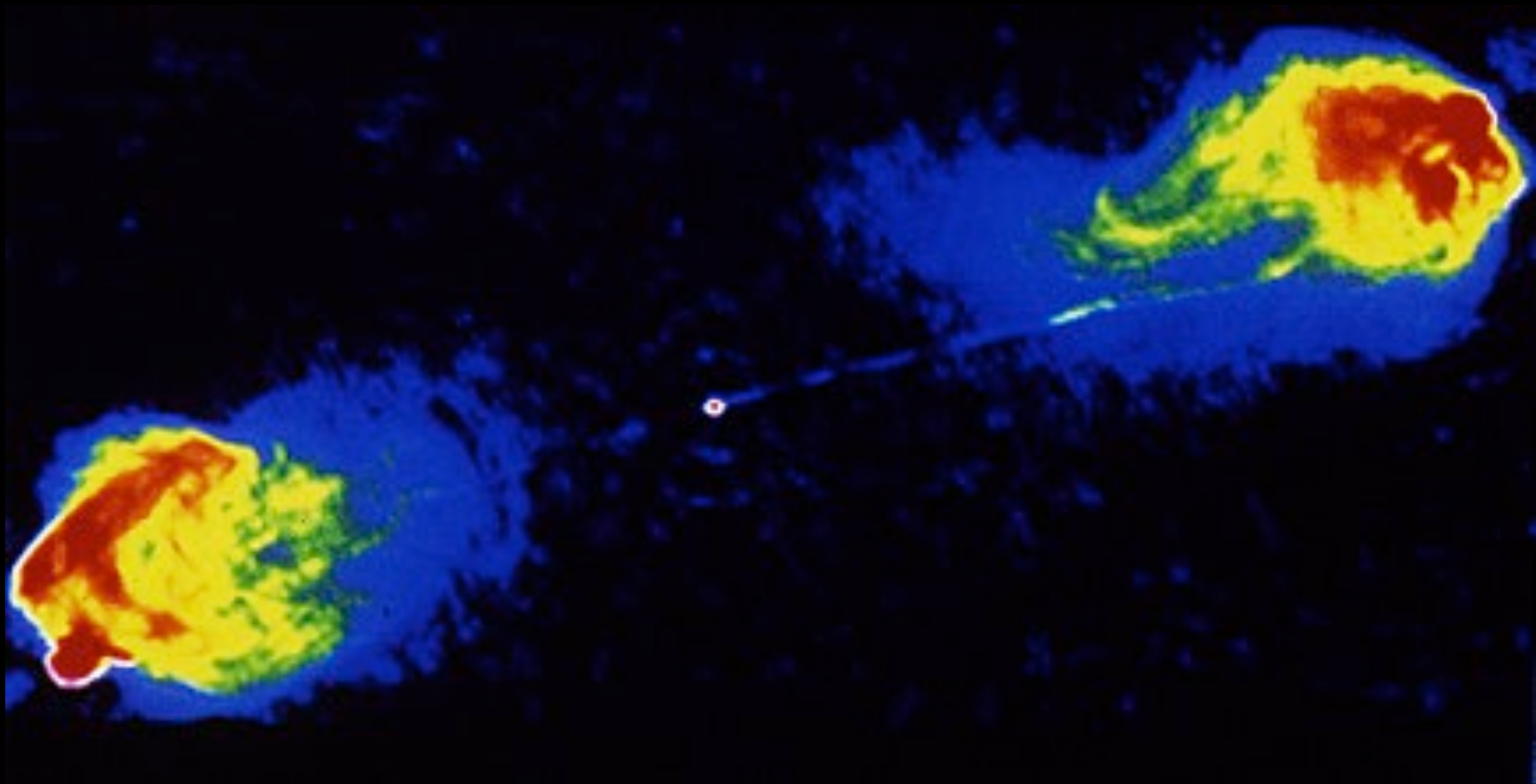

Cygnus A radio image
AGN


Centaurus A
AGN

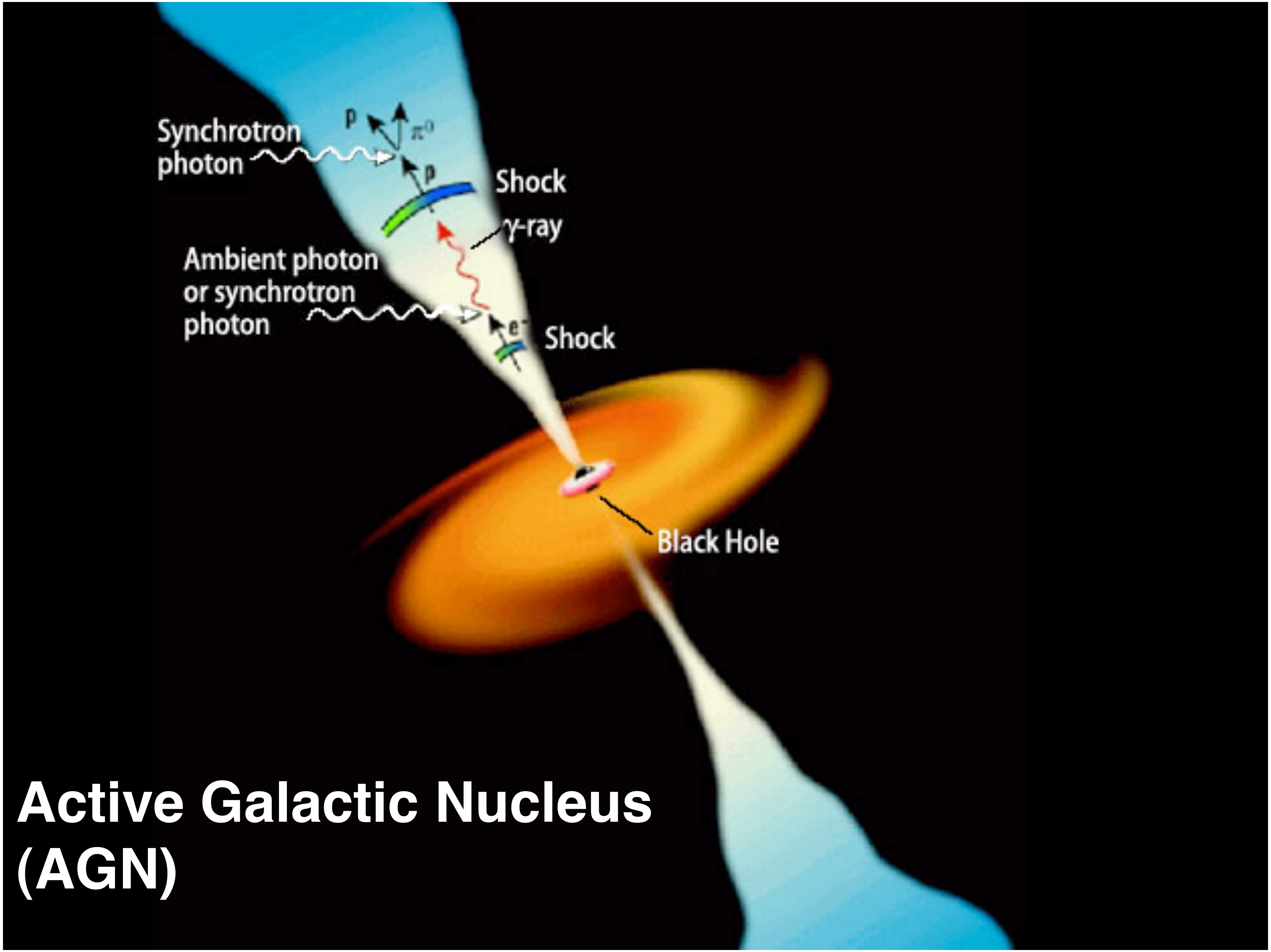

Active Galactic Nucleus (AGN)

the flow impinges on the external medium

the momentum moves the hotspots forward,
so that the lobes grow in size and luminosity

example for a typical radio galaxy: Cygnus A

$d = 170$ Mpc   two sperical regions, each
20 kpc in diameter

hot spots ~ 60 kpc from the parent galaxy

cm wavelength: $n = 0{,}75$ $\quad S \propto \nu^{-n}$

at 1 GHz radio luminosity $S = 4{,}3 \cdot 10^{27} \dfrac{W}{Hz}$

Radio Detection of Particles

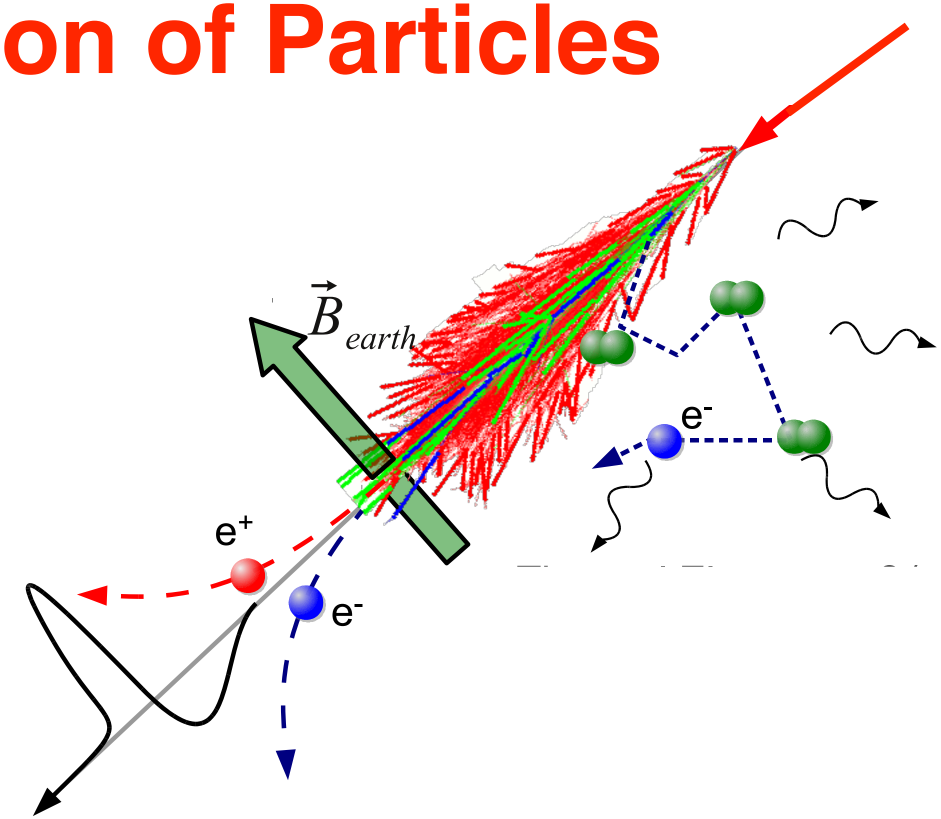

- **Cosmic Rays in atmosphere:**
  - **Geosynchrotron emission (10-100 MHz)**
  - **Radio fluorescence and Bremsstrahlung (~GHz)**
  - **Radar reflection signals (any?)**
  - **VLF emission, process unclear (<1 MHz)**
- **Neutrinos and cosmic rays in solids: Cherenkov emission (100 MHz - 2 GHz)**
  - **polar ice cap (balloon or in-ice)**
  - **inclined neutrinos through earth crust (radio array)**
  - **CRs and Neutrinos hitting the moon (telescope)**

Coherent Geosynchrotron Radio Emission

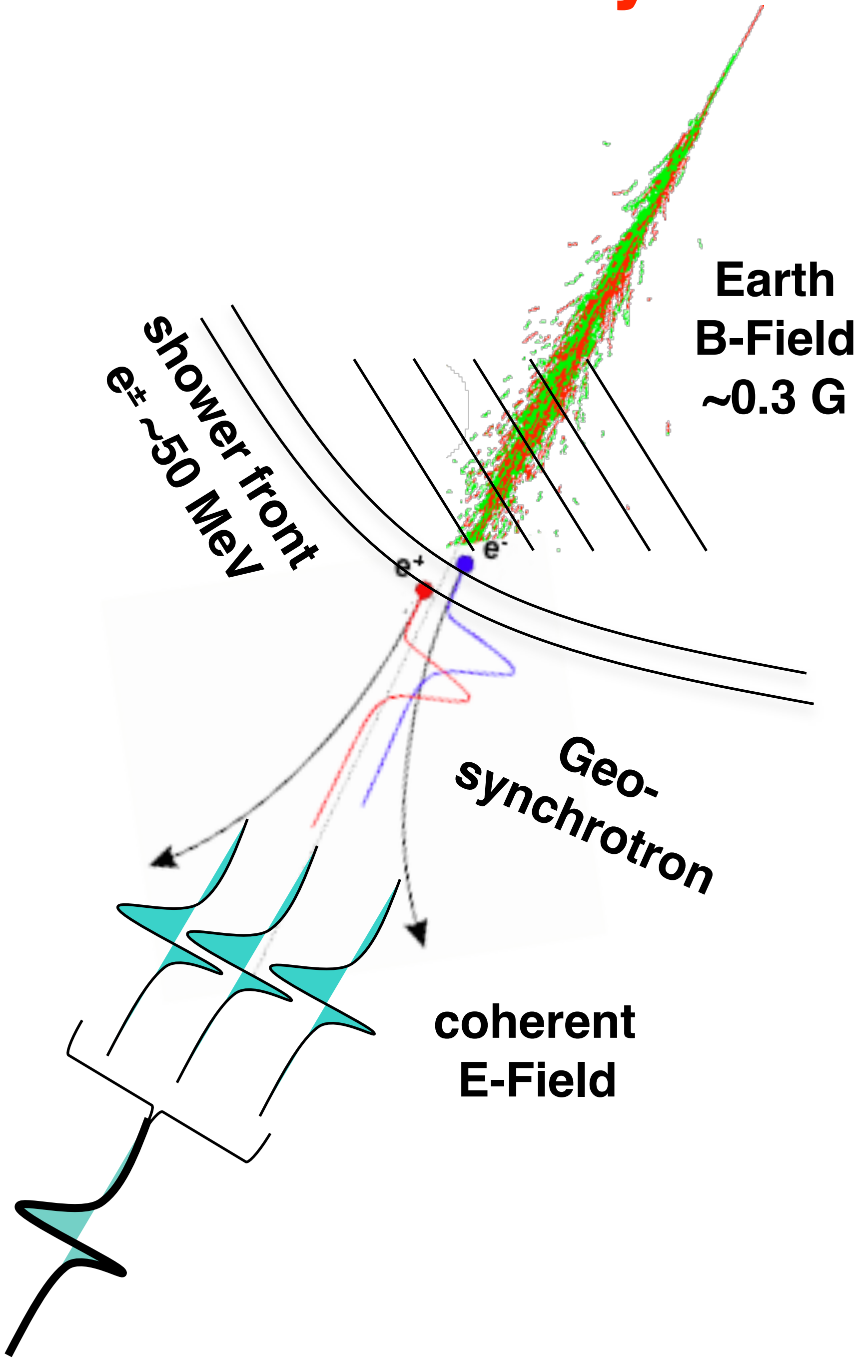

- UHECRs produce particle showers in atmosphere
- Shower front is ~2-3 m thick ~ wavelength at 100 MHz
- e± emit (mostly) synchrotron rad. in geomagnetic field
- Emissions from all e± (N_e) add up coherently
- Radio power grows quadratically with N_e

two contributions to signal

$$j' = (Q \cdot v)' = Q' \cdot v + Q \cdot v'$$

variation of total charge ~20%

synchrotron radiation ~80%

Large-scale radio detector to measure cosmic rays and neutrinos

LOPES

Radio Emission from Cosmic Ray Air Showers

0.5 km²

CODALEMA 0.5 km²

LOFAR

5 km² (core)

AERA

Auger Engineering Radio Array

20 km²

super Auger north

20 000 km²

LOPES
Lofar Prototype Station

30 antennas operating at KASCADE-Grande

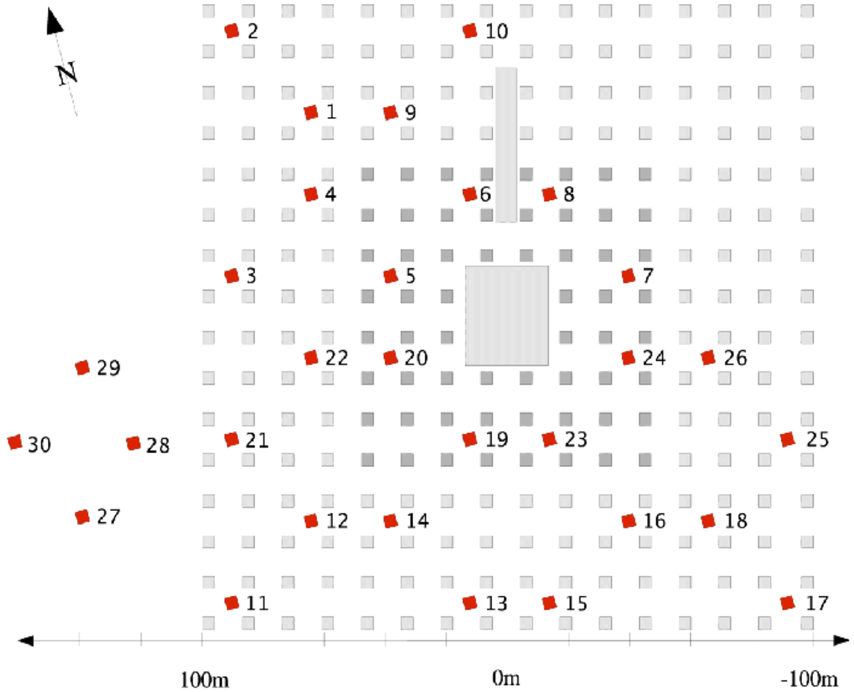

digital radio interferometer

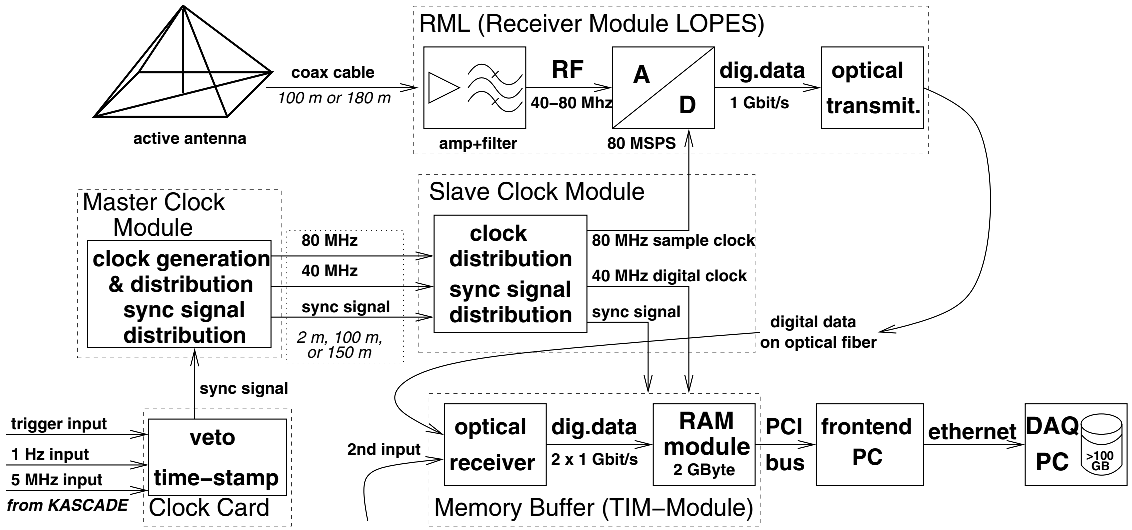

Proof of principle

LOPES-10

1. EAS properties (KASCADE)
2. radio signal analysis (cc beam)
3. sky map

Position of shower in sky

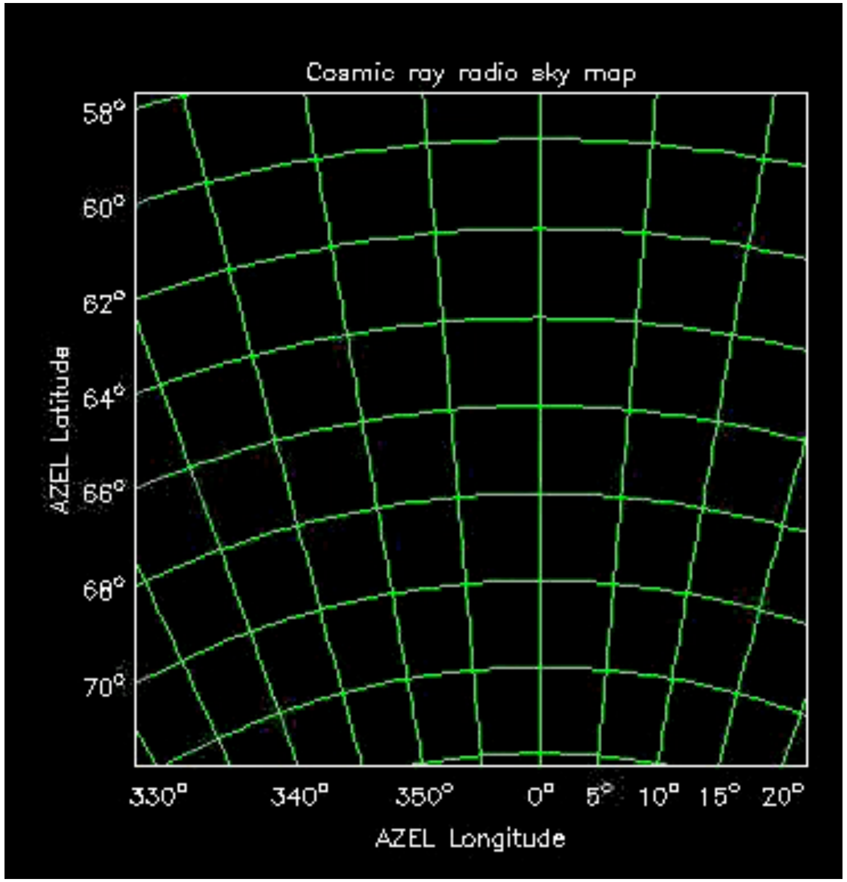

Nanosecond radio imaging in 3D

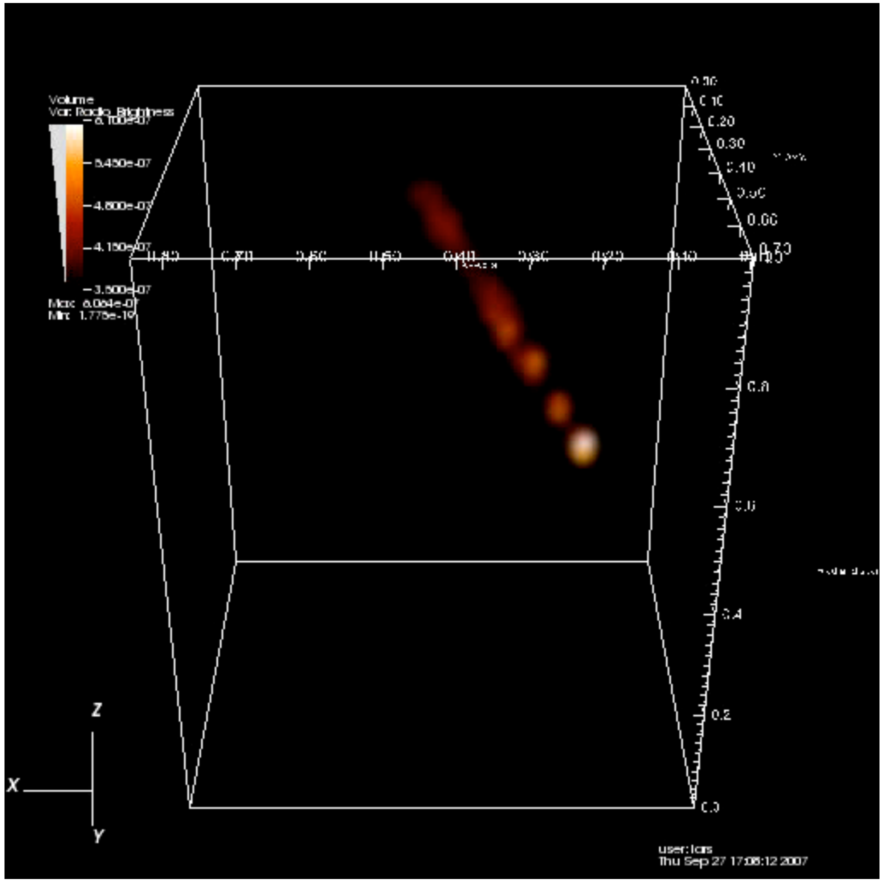

H. Falcke et al., Nature 435 (2005) 313

Correlation between radio signal and
air shower parameters

.. number of muons, i.e. primary energy

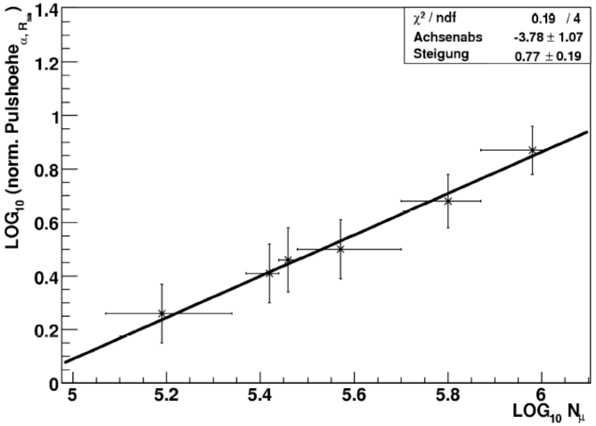

.. angle with respect to geomagnetic field

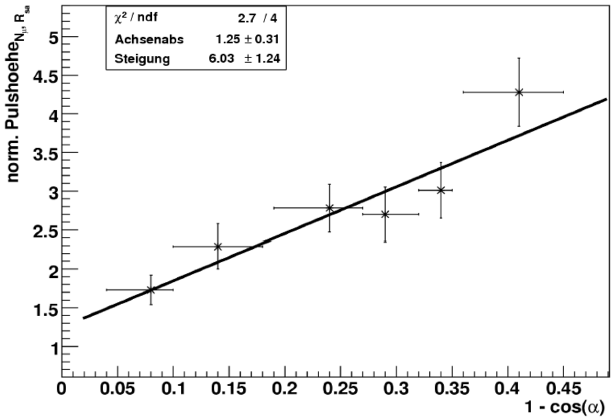

.. distance to shower axis

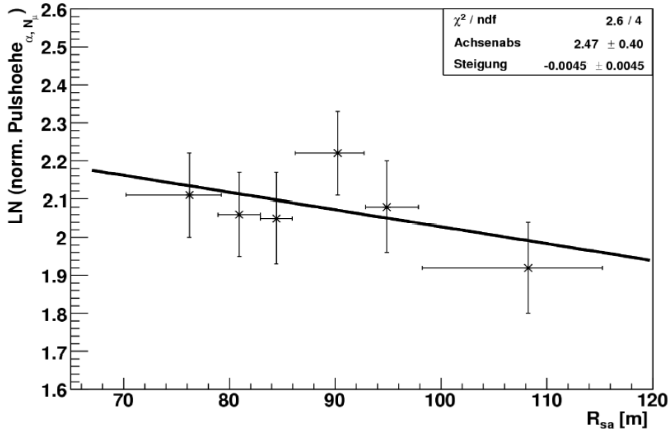

E. Bettini, diploma thesis, U Karlsruhe, 2006

$$\varepsilon_{est} = (11 \pm 1)((1.16 \pm 0.025) - \cos\alpha)\cos\theta \exp\left(\frac{-R}{236 \pm 81 \text{ m}}\right)\left(\frac{E_p}{10^{17} \text{ eV}}\right)^{0.95 \pm 0.04} \left[\frac{\mu\text{V}}{\text{m MHz}}\right]$$

α geomagnetic angle

θ zenith angle

r distance to shower axis

E_0 energy of primary particle

A. Horneffer et al., 30th ICRC 4 (2008) 83

LOPES: Polarization Measurements

arrival direction of cosmic rays (sky map)

E-W polarization

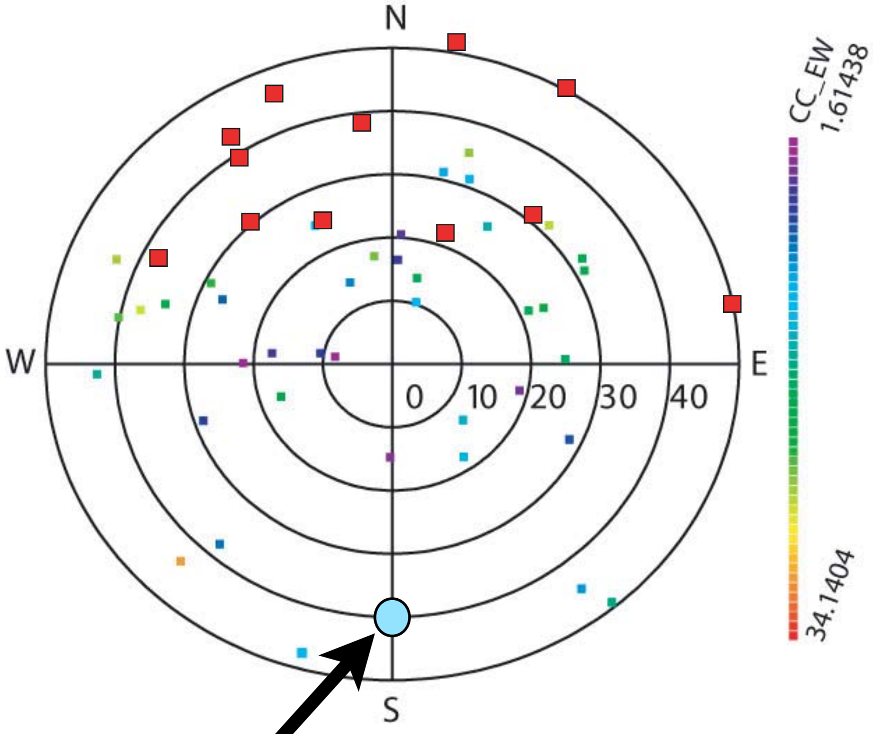

N-S polarization

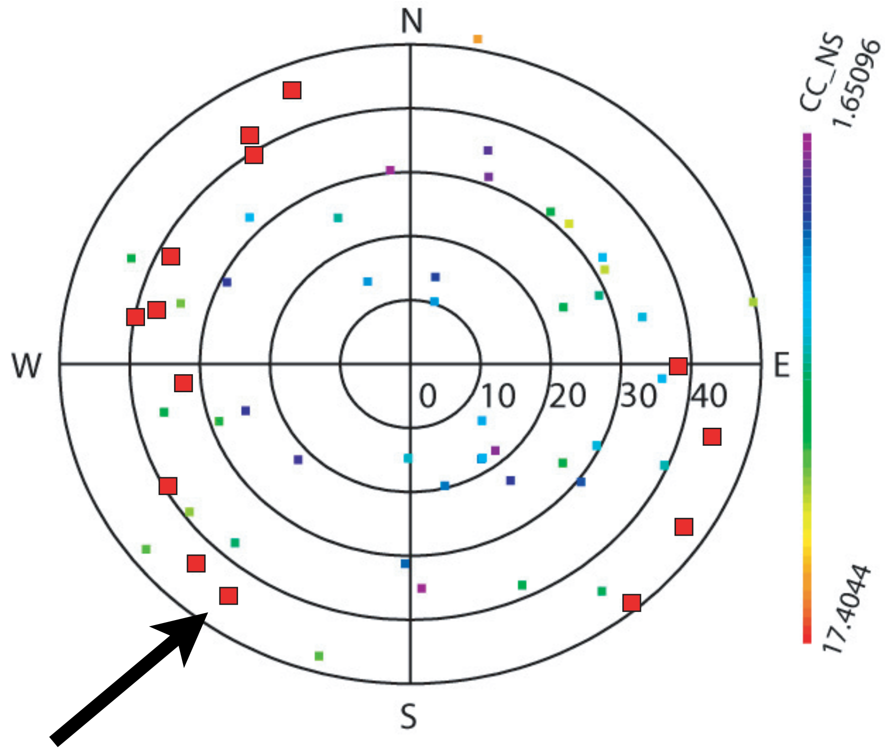

strongest events

magnetic field
inclination: 64° 36'
declination: 1° 22'

v x B effect
synchrotron radiation dominates signal

P.G. Isar et al., Nucl. Instr. & Meth. A 604(2009) S81

CODALEMA: shower arrival direction

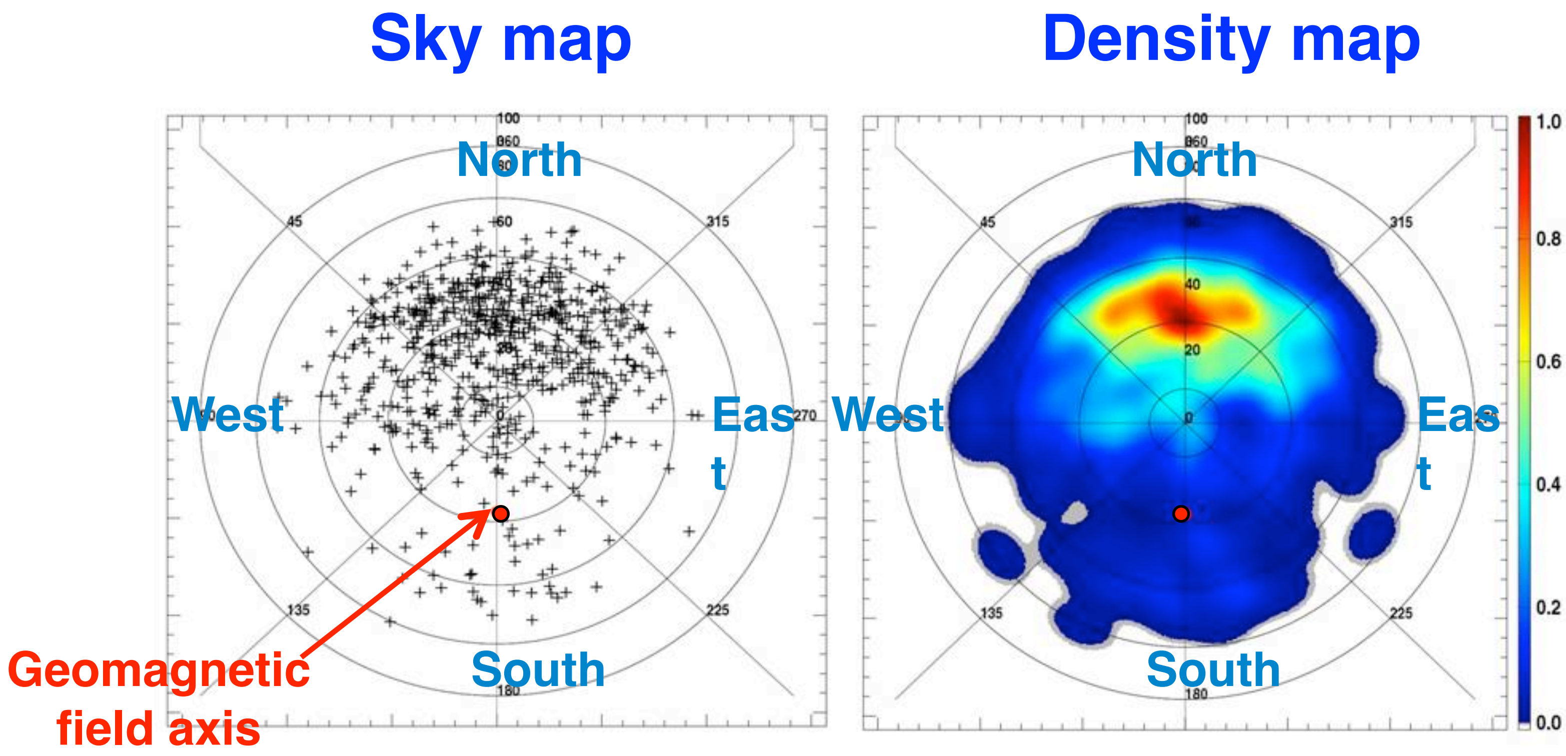

- **Large north/south asymmetry, relative deficit of events in the geomagnetic field axis area**

-**For the scintillators, the azimutal acceptance is uniform**

D. Arduin et al., Astropart. Phys. 31 (2009) 192

Synchrotron radiation of electrons (and positrons) in magnetic field of Earth

geosynchrotron radiation

general formula *(e.g. Jackson)* **for accelerated relativistic particle:**

$$E = \frac{e}{4\pi\epsilon_0}\left[\frac{n-v}{\gamma^2(1-v\cdot n)^3R^2}\right]_{ret} + \frac{e}{4\pi\epsilon_0 c}\left[\frac{n\times\{(n-v)\times\dot{v}\}}{(1-v\cdot n)^3R}\right]_{ret}$$

v **velocity of particle**

n **direction of observer**

second term represents synchrotron emission when

$$\dot{v} = \frac{e}{\gamma m} v \times B$$ **Lorentz acceleration in magnetic field**

geosynchrotron radiation

$$E = \frac{e}{4\pi\epsilon_0}\left[\frac{n-v}{\gamma^2(1-v\cdot n)^3R^2}\right]_{ret} + \frac{e}{4\pi\epsilon_0 c}\left[\frac{n\times\{(n-v)\times\dot{v}\}}{(1-v\cdot n)^3R}\right]_{ret}$$

assume: observation point on shower axis $v \,||\, n$

$$\Rightarrow E_2 \propto n\times\{(n-v)\times(v\times B)\}$$

$$\propto \underbrace{\{n(v\times B)\}}_{=0 \text{ on axis}}(n-v) - \{n(n-v)\}\,(v\times B)$$

$$\propto -(1-v)(v\times B)$$

$$\propto -(v\times B)$$

geosynchrotron radiation

field strength of observed radiation is expected as

$$E \propto -(v \times B)$$

total field amplitude

in experiments, projection on E-W or N-S direction is measured

CODALEMA: Geomagnetic Origin v x B

A model to understand the asymmetry

Hypothesis:

- The electric field is proportional to the Lorentz force E ~ |v x B|
    - Charged particles in the shower are deflected by the geomagnetic field
    - Electric field polarization in the direction of the Lorentz force :
      a linear polarization is assumed E // to v x B
- The number of count (i.e. the efficiency) depends on the electric field magnitude:
      a simple linear dependence is assumed

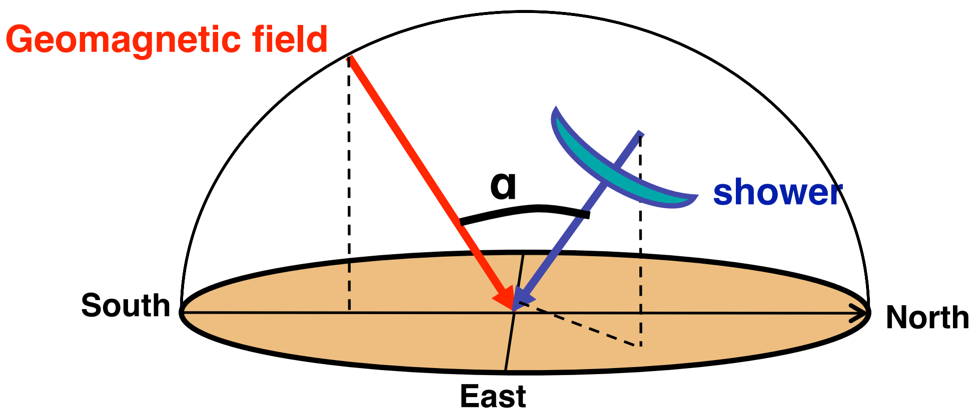

D. Arduin et al., Astropart. Phys. 31 (2009) 192

CODALEMA: Geomagnetic Origin v x B

sky map of radio events (E-W component)

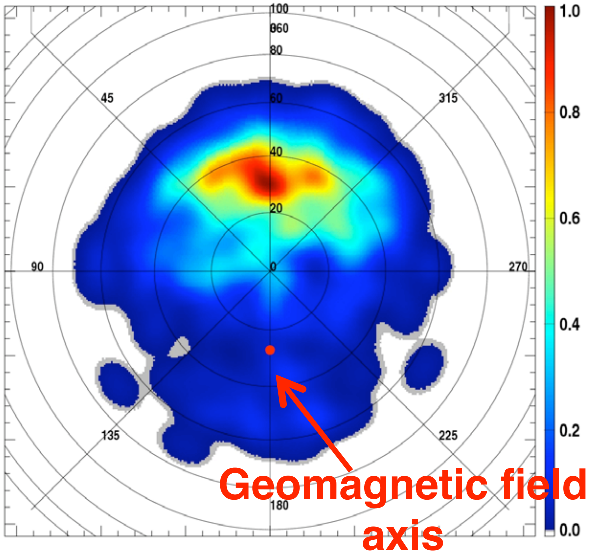

measured

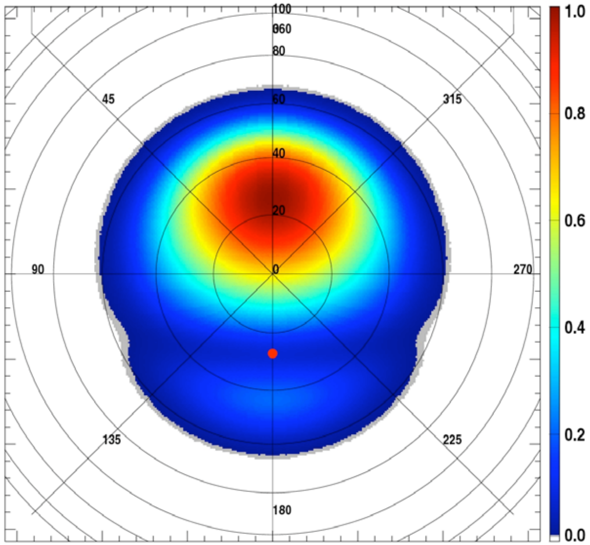

simulated

asymmetry of observed events

Lorentz force $\vec{v} \times \vec{B}$

v direction of shower axis
B direction of Earth magnetic field

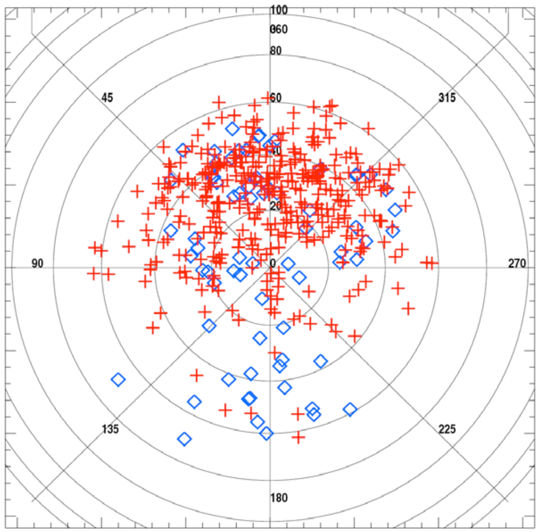

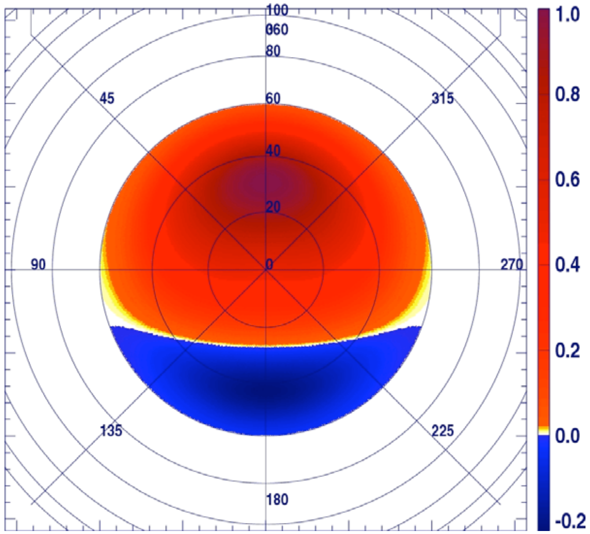

polarity of electric field

geomagnetic origin

D. Arduin et al., Astropart. Phys. 31 (2009) 192

Station Layout

130 m

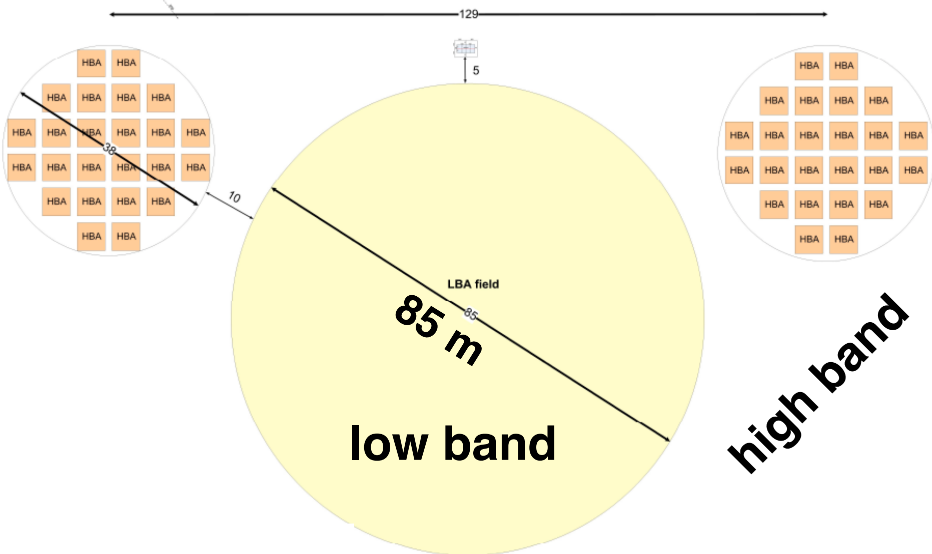

each (dutch) station:

96 low-band antennae 30- 80 MHz

high-band antennae (2x24 tiles) 120-240 MHz

high band

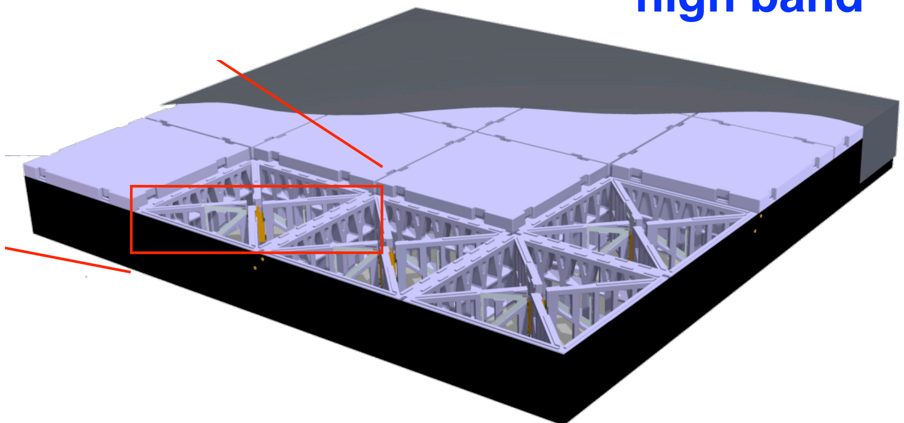

www.lofar.org

LOFAR Radboud Air Shower Array - LORA

20 scintillator stations
(~1 m² each)
read out by wavelength
shifter bar and PMT
in LOFAR core

▶ provide basic information on EAS and trigger

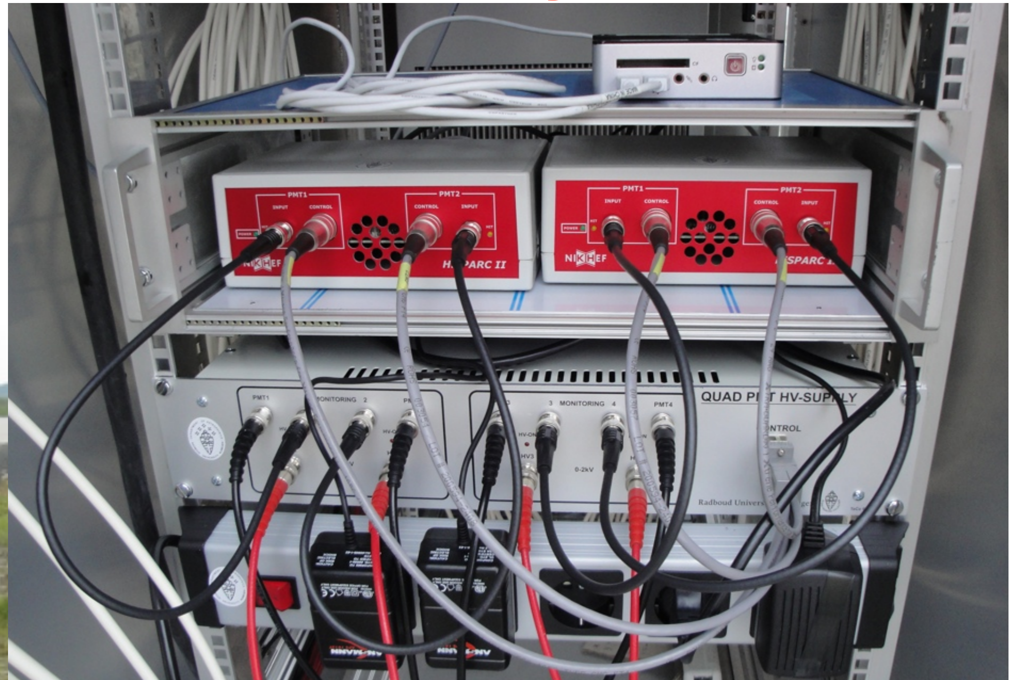

Sky map of TBB triggers

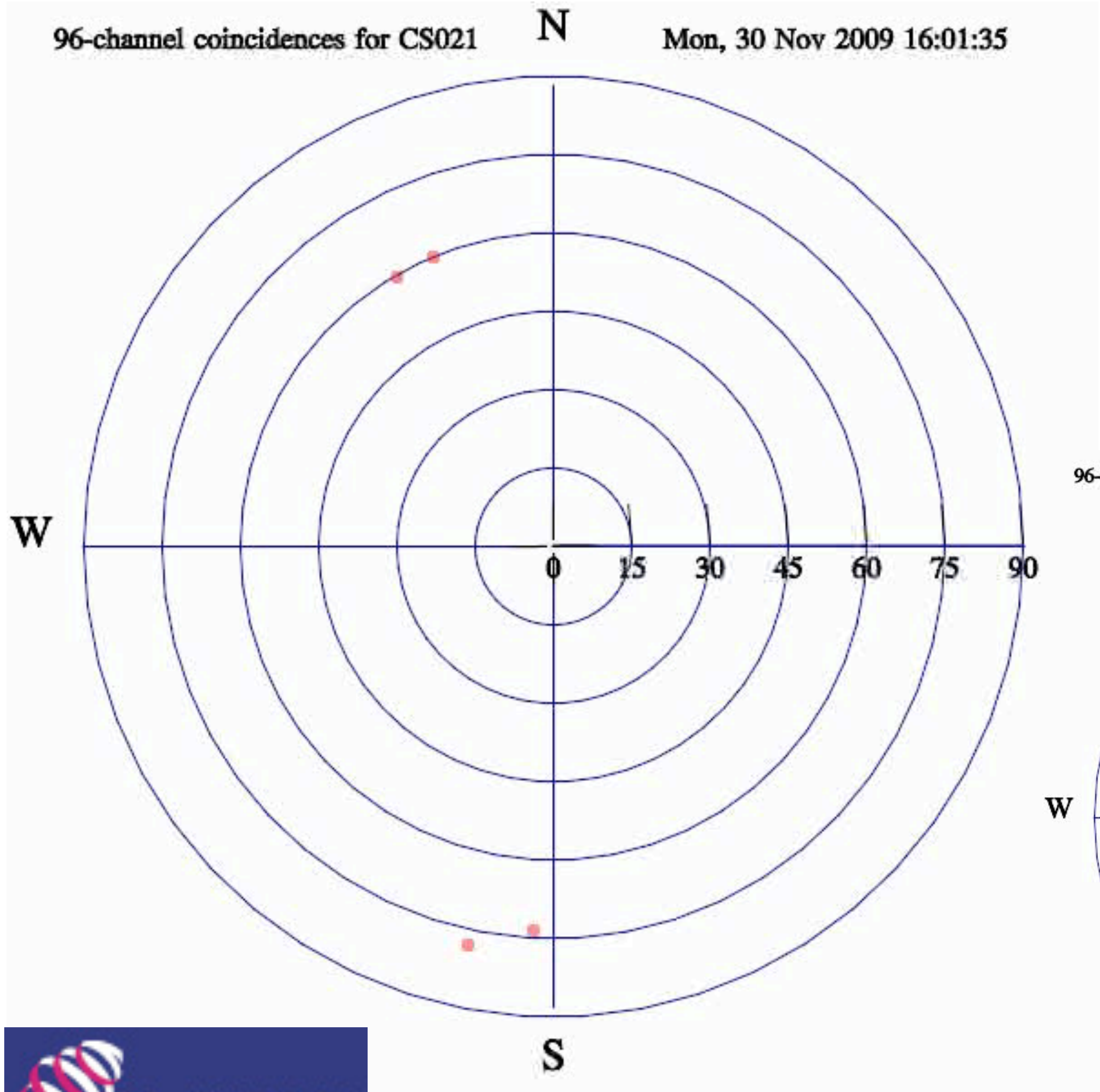

airplane

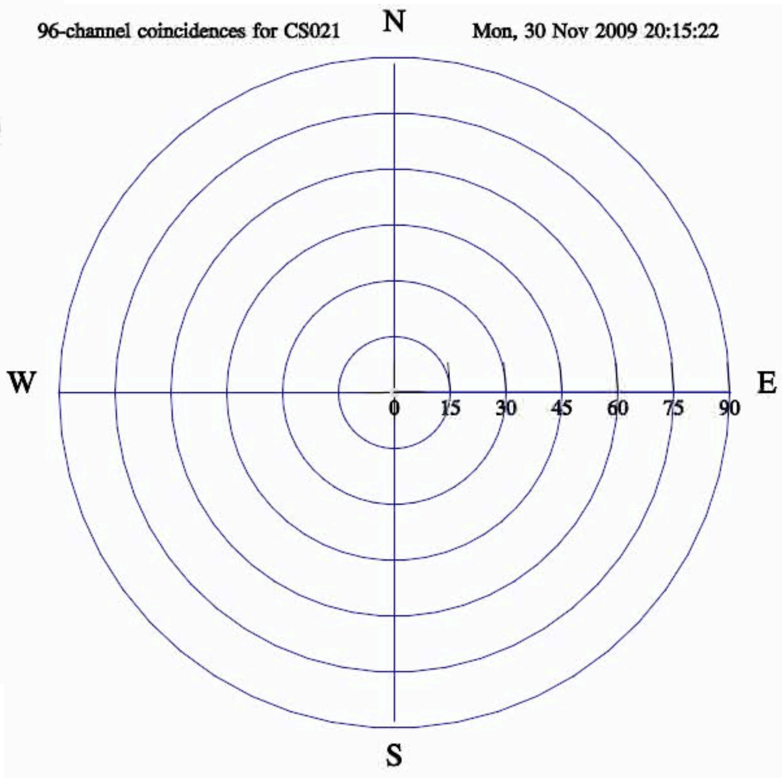

LOFAR

AERA
Auger Engineering Radio Array

Objective:

- measure radio emission from EAS in frequency range 30 MHz - 80 MHz
- ~20 km² array with ~160 antennas
- operation together with infill/HEAT/AMIGA
- three antenna spacings to cover efficiently 17.2 < lg E/eV < 19.0
- measure composition of cosmic rays in energy region of transition from galactic to extragalactic cosmic rays

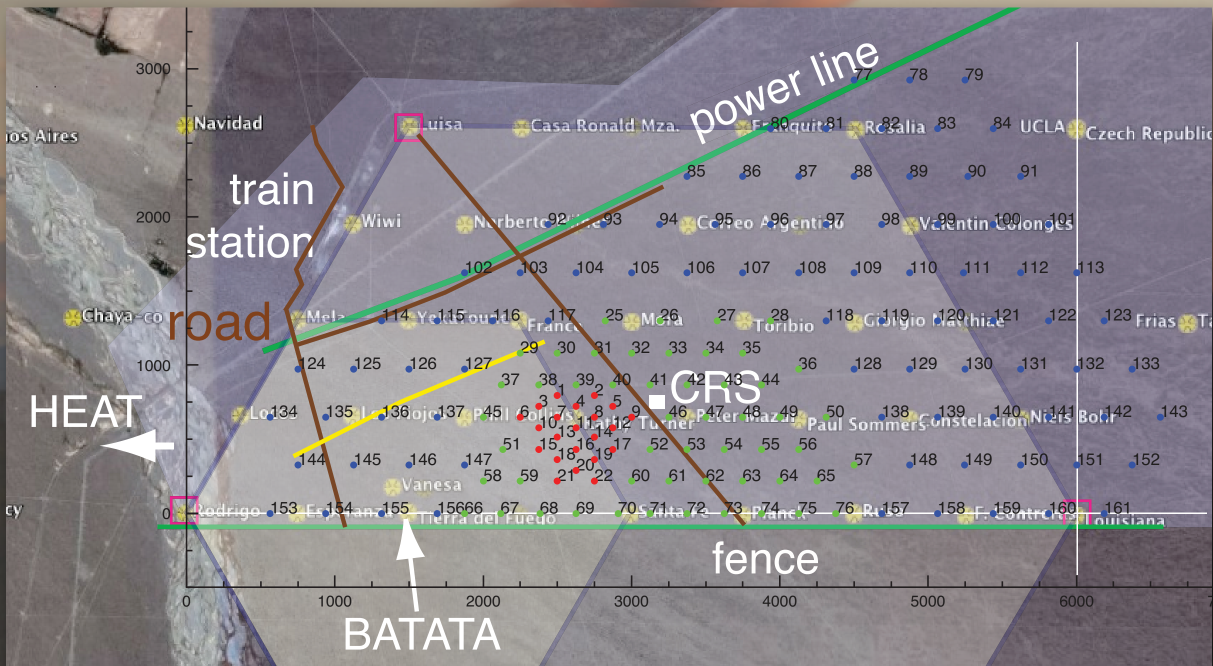

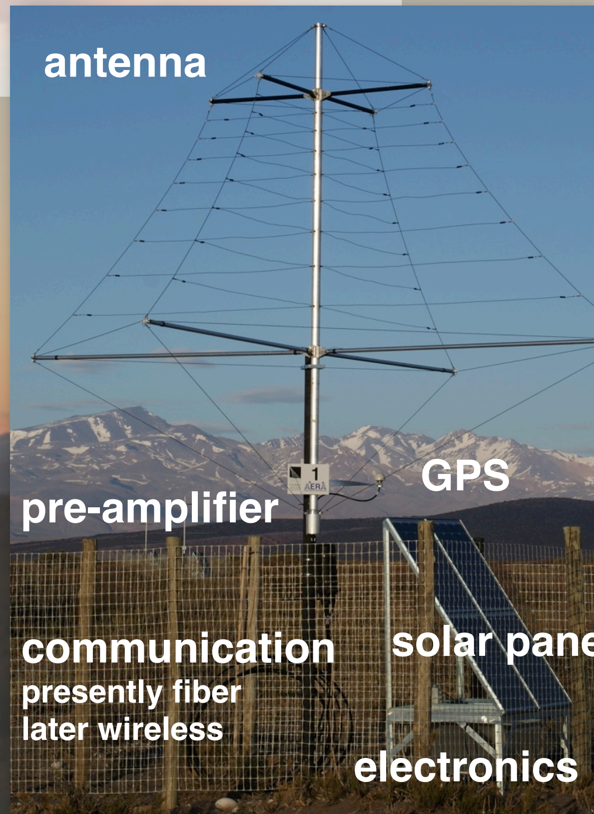


AERA
Auger Engineering Radio Array
22 stations installed and taking data

Sidereal Modulation of Galactic Noise

NS Channel, one station 10 s traces, Oct 8th - Oct 13th

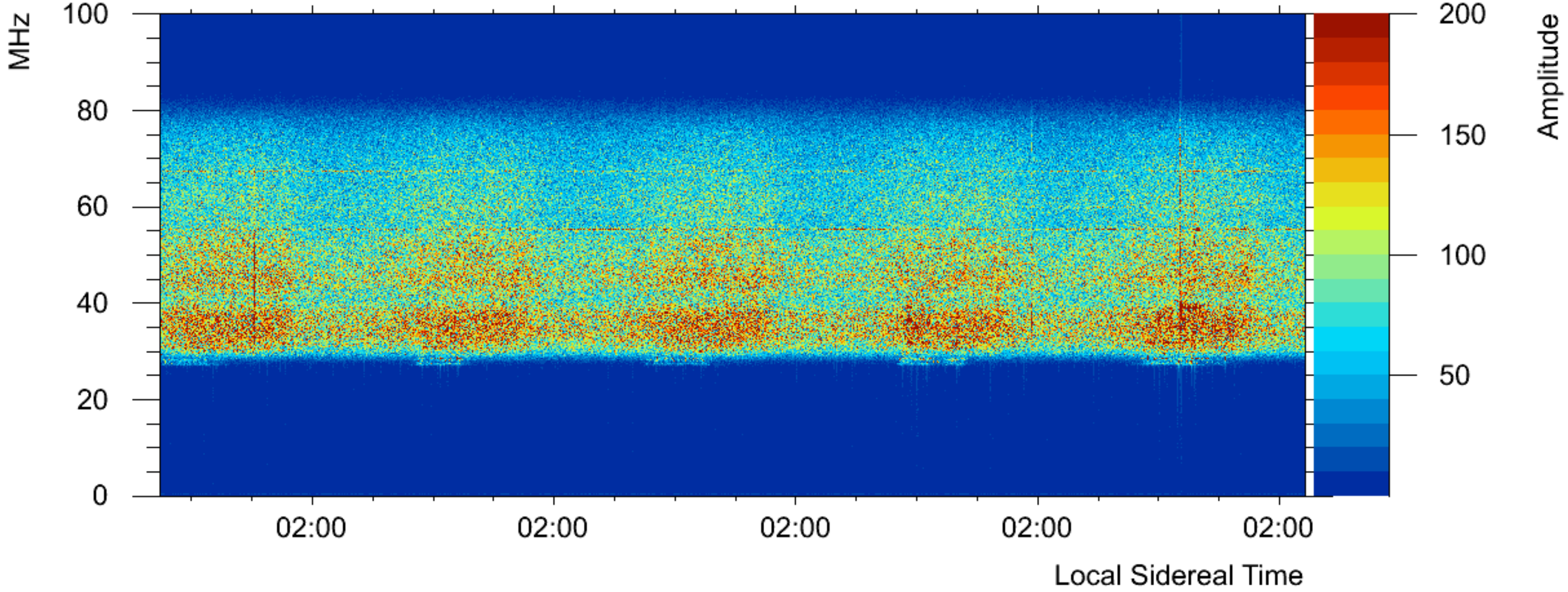

Rise of Galactic Center: LST 10:10
Maximum: LST 17:45
Set of Galactic Center: LST 01:15

Test measurements at Auger: short dipoles

event density on ground

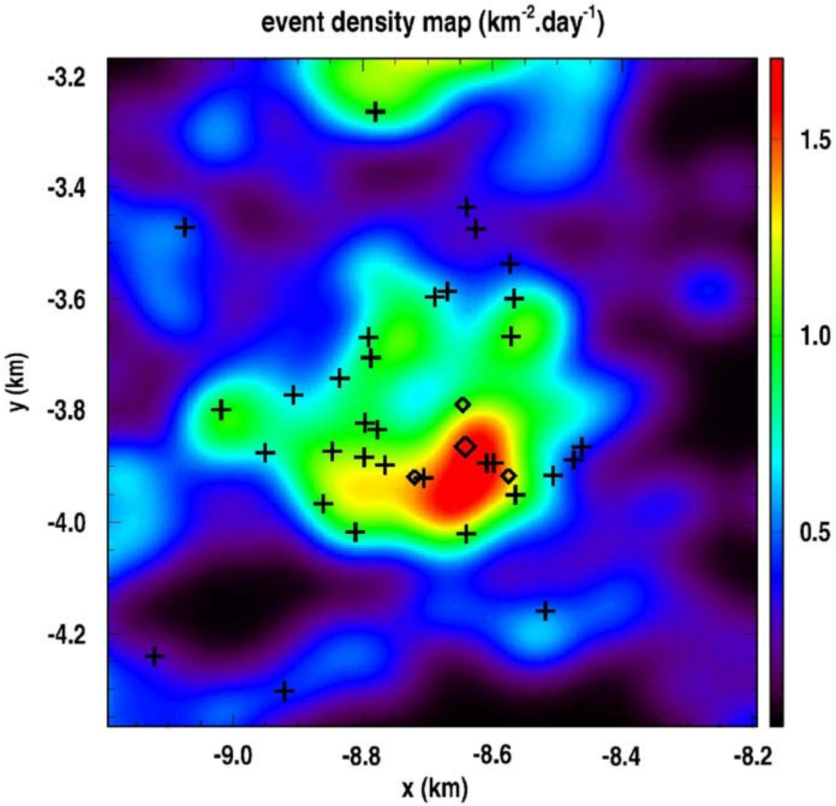

Fig. 4. Event ground density map around Apolinario, computed from the official Auger event list and smoothed by a 50 m width Gaussian. The color scale is in number of events m^{-2} day^{-1}. The Auger events with a radio counterpart are indicated by the black crosses. Apolinario is the largest diamond at the center and the three radio stations are the smallest diamonds around.

sky map

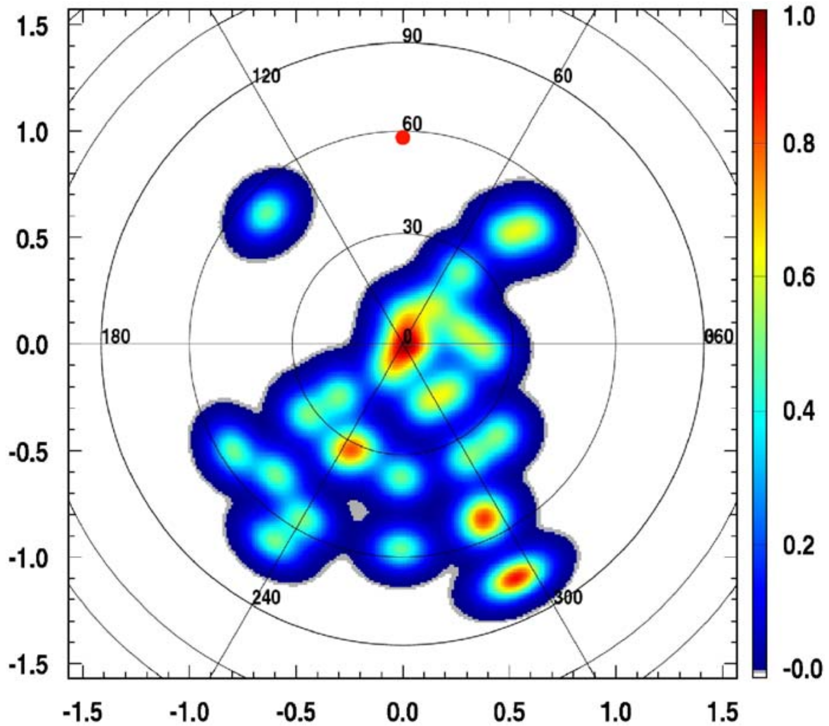

Fig. 5. Sky map in local coordinates of the radio events seen in coincidence with Auger SD and smoothed by a 10° Gaussian beam. The zenith is at the center, North at the top, East on the right. The 75.8% of the events are coming from the South while the Auger SD events sky map is uniform in azimuth. The red dot towards the north at $\theta \sim 58^{\circ}$ is the location of the geomagnetic field in Malargüe. (For interpretation of the references to color in this figure legend, the reader is referred to the web version of this article.)

PIERRE AUGER OBSERVATORY

AERA Auger Engineering Radio Array

B. Revenu, Nucl. Instr. & Meth. A 604 (2009) S37

Sky plot of reconstructed events

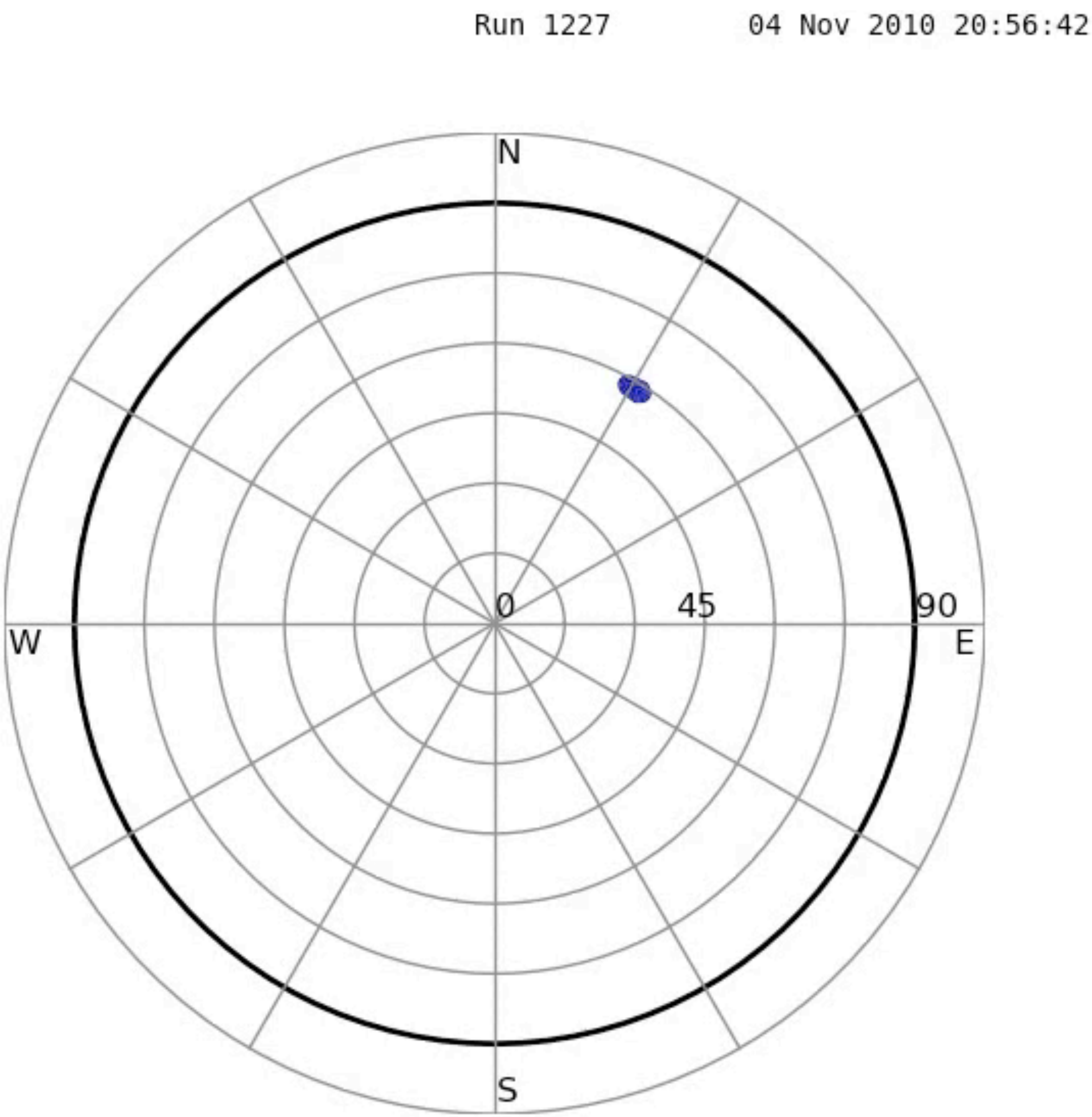

Directions of the noise sources

El Sosneado, Communication Tower ?

Farms, Oil ?

El Diamante ?

???

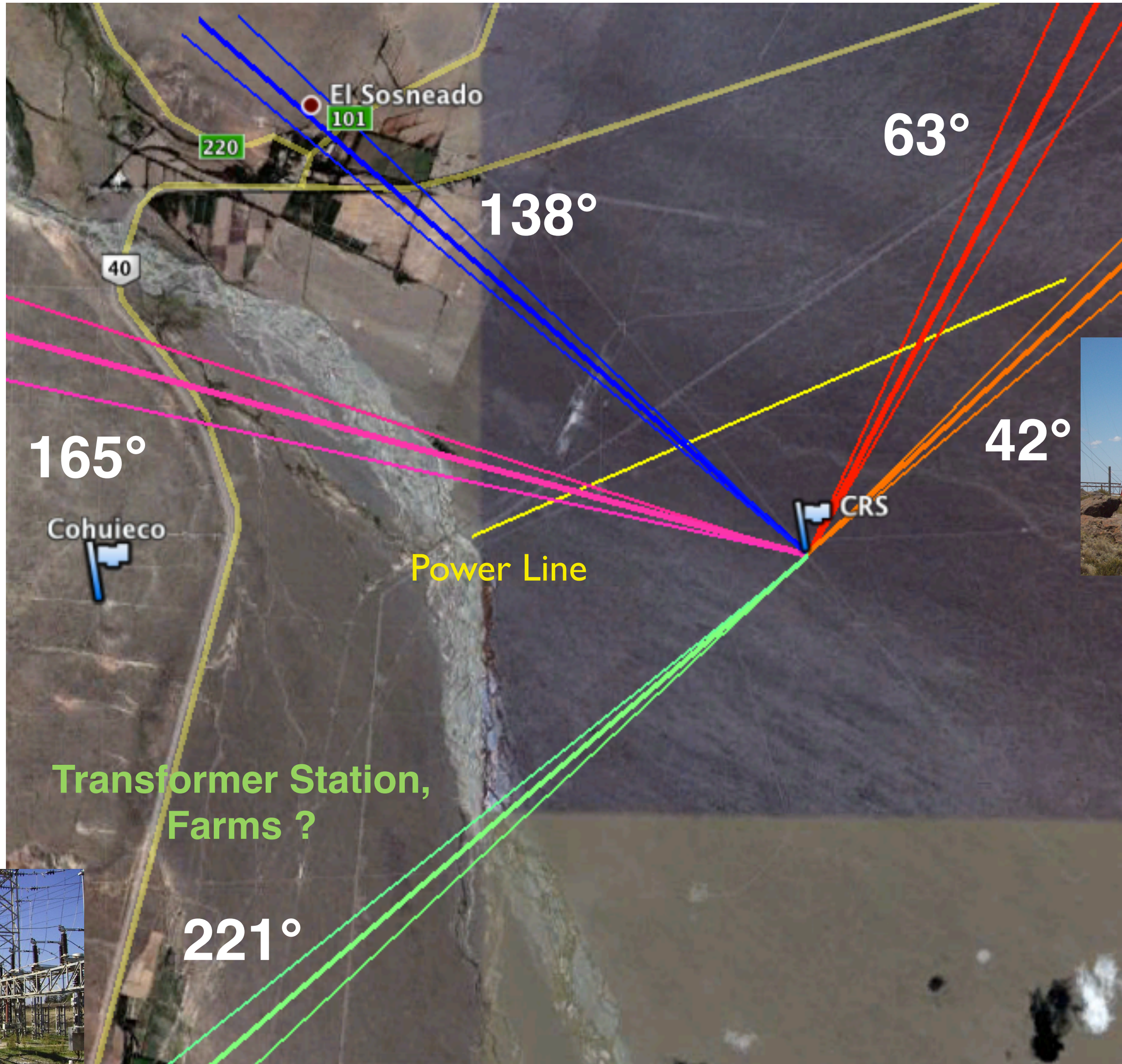

Antennas at El Diamante

AERA Auger Engineering Radio Array

Sky plot of reconstructed events

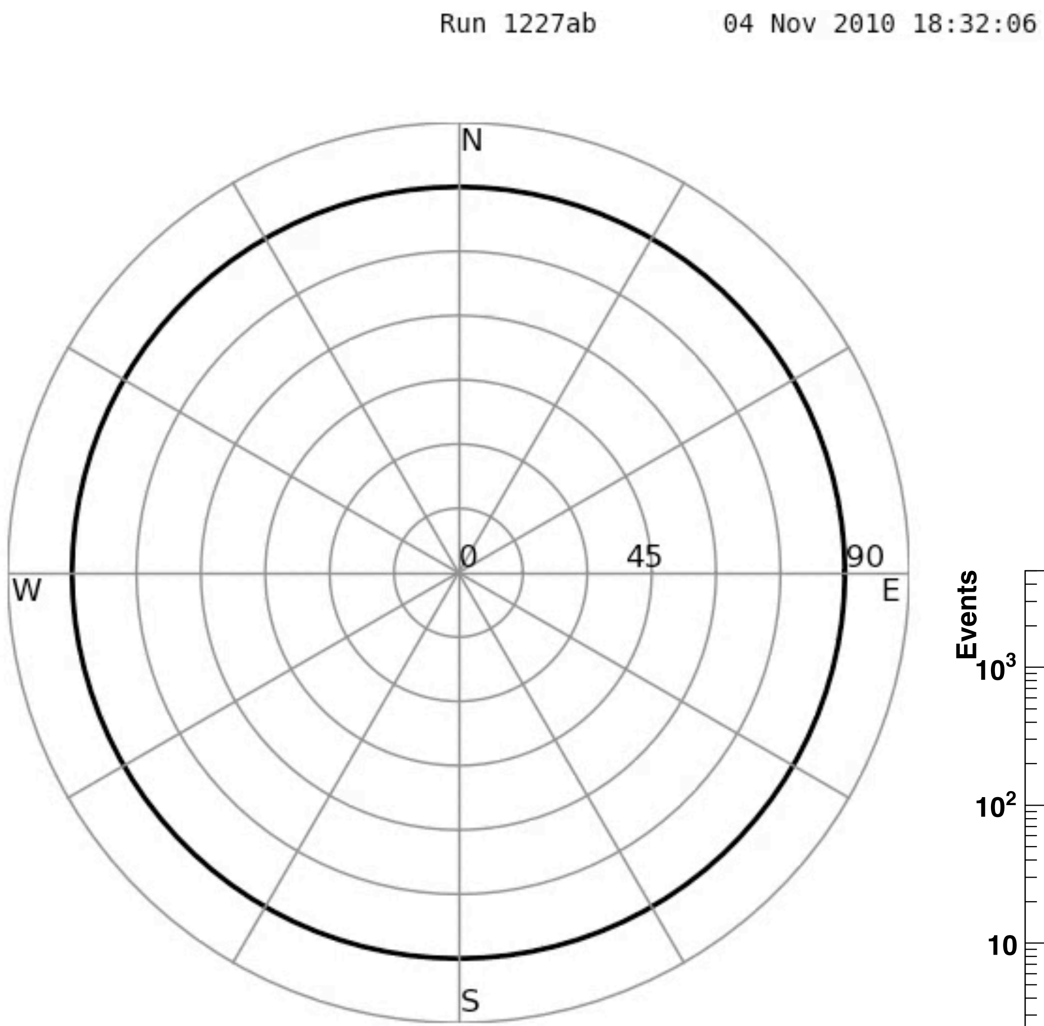

zenith angle < 60°

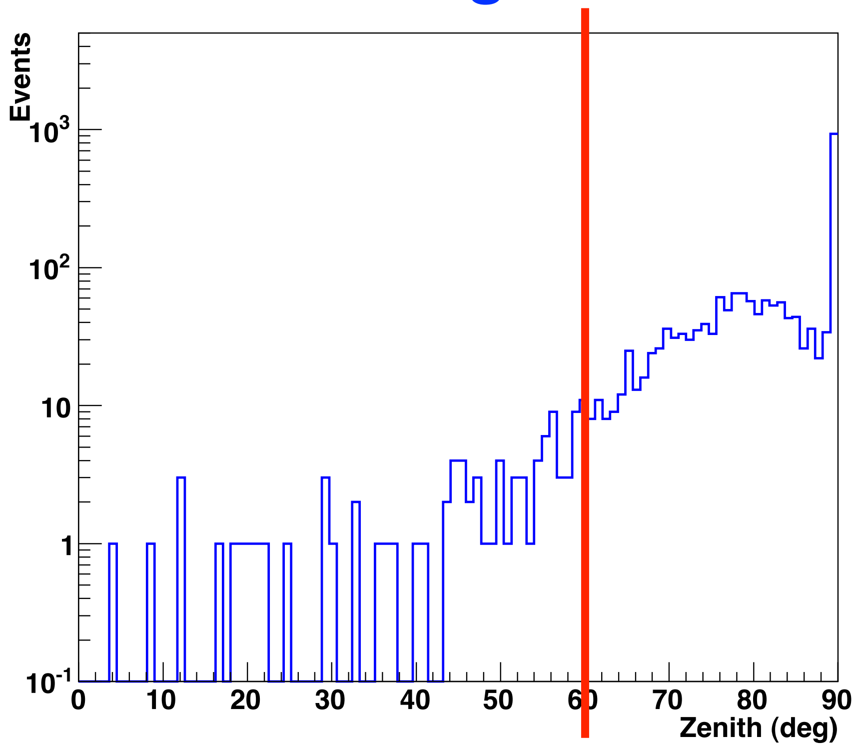

noise from horizon

„the sky is clean“

signals from EAS expected soon